The complexity of millennial-scale variability in southwestern Europe during MIS 11

Article · November 2016

DOI: 10.1016/j.yqres.2016.09.002

10 authors, including:

Filipa Naughton
Instituto Português do Mar e da Atmosfera

Ricardo M Trigo
University of Lisbon

Cristina Lopes
Instituto Português do Mar e da Atmosfera

Maria Fernanda Sanchez Goñi
Ecole Pratique des Hautes Etudes

Quaternary Research xxx (2016) 1–15

Contents lists available at ScienceDirect

Quaternary Research

journal homepage: http://www.journals.elsevier.com/quaternary-research

The complexity of millennial-scale variability in southwestern Europe during MIS 11

Dulce Oliveira [a, b, c, d, *], Stéphanie Desprat [a, b], Teresa Rodrigues [c, d], Filipa Naughton [c, d], David Hodell [e], Ricardo Trigo [f], Marta Rufino [c, d], Cristina Lopes [c, d], Fátima Abrantes [c, d], Maria Fernanda Sánchez Goñi [a, b]

[a] EPHE, PSL Research University, Laboratoire Paléoclimatologie et Paléoenvironnements Marins, F-33615 Pessac, France
[b] Univ. Bordeaux, EPOC, UMR 5805, F-33615 Pessac, France
[c] Divisão de Geologia e Georecursos Marinhos, Instituto Português do Mar e da Atmosfera (IPMA), Avenida de Brasília 6, 1449-006 Lisboa, Portugal
[d] CCMAR, Centro de Ciências do Mar, Universidade do Algarve, Campus de Gambelas, 8005-139 Faro, Portugal
[e] Godwin Laboratory for Palaeoclimate Research, Department of Earth Sciences, University of Cambridge, UK
[f] Instituto Dom Luiz, Universidade de Lisboa, 1749-016 Lisboa, Portugal

ARTICLE INFO

Article history:
Received 11 February 2016
Available online xxx

Keywords:
Marine Isotope Stage (MIS) 11
Iberian margin
Mediterranean vegetation
Millennial-scale climate variability
Cooling events
Land–sea comparison
Pollen analysis

ABSTRACT

Climatic variability of Marine Isotope Stage (MIS) 11 is examined using a new high-resolution direct land–sea comparison from the SW Iberian margin Site U1385. This study, based on pollen and biomarker analyses, documents regional vegetation, terrestrial climate and sea surface temperature (SST) variability. Suborbital climate variability is revealed by a series of forest decline events suggesting repeated cooling and drying episodes in SW Iberia throughout MIS 11. Only the most severe events on land are coeval with SST decreases, under larger ice volume conditions. Our study shows that the diverse expression (magnitude, character and duration) of the millennial-scale cooling events in SW Europe relies on atmospheric and oceanic processes whose predominant role likely depends on baseline climate states. Repeated atmospheric shifts recalling the positive North Atlantic Oscillation mode, inducing dryness in SW Iberia without systematical SST changes, would prevail during low ice volume conditions. In contrast, disruption of the Atlantic meridional overturning circulation (AMOC), related to iceberg discharges, colder SST and increased hydrological regime, would be responsible for the coldest and driest episodes of prolonged duration in SW Europe.

Introduction

The Mediterranean region is particularly sensitive to global climate change owing to its geographical position between the mid-latitudes and subtropical climate regimes (Giorgi, 2006; Lionello et al., 2006; IPCC, 2013). Climate projections show repeated occurrence of severe drought episodes in the Mediterranean area, including the Iberian Peninsula, which will deeply affect terrestrial ecosystems (Gao and Giorgi, 2008; Anav and Mariotti, 2011; Santini et al., 2014; Sousa et al., 2015a). During past climatic cycles, it has been demonstrated that similar recurring dry conditions led to drastic forest decline in southern Europe. However, while millennial-scale climate variability has been widely documented mainly for the last glacial period (e.g., Sánchez Goñi et al., 2000, 2008; Combourieu-Nebout et al., 2002; Fletcher and Sánchez Goñi, 2008; Naughton et al., 2009; Fletcher et al., 2010), few available records report abrupt interglacial climate variability prior to the current interglacial.

Specifically, Marine Isotope Stage (MIS) 11 (425–374 ka) represents a period of primary interest to investigate natural abrupt climate variability. Despite its potential astronomical analogy with the Holocene (Loutre and Berger, 2003) remaining complex and controversial (e.g., Tzedakis, 2010; Yin and Berger, 2012), this interglacial presents additional key features, including its higher than present-day sea level related to the collapse of Greenland and West Antarctica ice sheets (Raymo and Mitrovica, 2012; Roberts et al., 2012; Reyes et al., 2014) and its greenhouse gas-driven climate warming (Raynaud et al., 2005; Yin and Berger, 2012).

* Corresponding author. EPHE, PSL Research University, Laboratoire Paléoclimatologie et Paléoenvironnements Marins, F-33615 Pessac, France.
E-mail address: dulce.oliveira@ipma.pt (D. Oliveira).

http://dx.doi.org/10.1016/j.yqres.2016.09.002
0033-5894/

MIS 11c generally stands out as a long, warm and relatively stable interglacial in numerous records (e.g., Oppo et al., 1998; McManus et al., 2003; Bauch, 2012; Melles et al., 2012; Milker et al., 2013; Candy et al., 2014), although few high temporal resolution records from Antarctica, subtropical and subpolar North Atlantic, and northern Europe, document pronounced abrupt climate change during MIS 11c despite reduced ice caps (Oppo et al., 1998; Billups et al., 2004; Koutsodendris et al., 2011; Pol et al., 2011; Tye et al., 2016). Comparatively, suborbital climatic variability during MIS 11b (~395–374 ka) is well documented in records from the North Atlantic, particularly off western Iberia (de Abreu et al., 2005; Martrat et al., 2007; Stein et al., 2009; Voelker et al., 2010; Rodrigues et al., 2011; Amore et al., 2012; Palumbo et al., 2013; Hodell et al., 2013a; Marino et al., 2014; Maiorano et al., 2015). Three marked cooling episodes linked to deep ocean circulation changes and iceberg discharges into the North Atlantic are commonly reported (e.g., Oppo et al., 1998). Yet, the amplitude of precipitation, changes in temperature and duration of the cold episodes on land associated with these abrupt changes are not well known. In addition, phase relationship between ocean and terrestrial climatic changes remain to be assessed since air–sea decoupling was identified during some periods of ice sheet growth by European margin records (Sánchez Goñi et al., 2013; Cortina et al., 2015). So far, only two pollen records have been published in the northern and southern parts of the Iberian margin for MIS 11 (Desprat et al., 2005; Tzedakis et al., 2009). However, the temporal resolution of these records precludes a reliable assessment of the regional vegetation-based climate in response to the millennial-scale cooling throughout MIS 11.

Although millennial-scale variability is an inherent pattern of the Pleistocene climate regardless of glacial state (Oppo et al., 1998), ice sheet dynamics is one of the primary factors modulating millennial-scale cooling events. Cooling episodes in the North Atlantic associated with iceberg surges would be amplified when ice sheet size surpasses a critical threshold (McManus et al., 1999). Freshwater from melting icebergs may be responsible for the enhancement and/or prolonged duration of cold conditions through a positive feedback mechanism on AMOC (Atlantic Meridional Overturning Circulation) even if they may not be the trigger of northern stadial events (Barker et al., 2015). However, the duration and intensity of northern cold events may also rely on the background climate, such as the intensity of regional precipitation, modifying the AMOC response to freshwater forcing (Margari et al., 2010). To date, the factors modulating millennial-scale cooling of MIS 11 remain insufficiently understood.

Here we present a new high resolution record of MIS 11 from Site U1385, also known as the "Shackleton Site", collected recently during the Integrated Ocean Drilling Program (IODP) Expedition 339. Site U1385 is located on the SW Iberian margin (Fig. 1), considered as a unique and exceptional area for paleoclimate research since Nick Shackleton's seminal study of the last climatic cycle recorded at the nearby site MD95-2042 (Shackleton et al., 2000, 2004), and the publication of the first direct land–sea comparison from the same site (Sánchez Goñi et al., 1999, 2000; Shackleton et al., 2003). We provide a detailed record of atmospherically-driven southern European vegetation changes at suborbital time scales that we directly compare with sea surface temperatures in eastern subtropical North Atlantic. Cooling events, differing in terms of magnitude, character and duration, are discussed in the light of a larger European and North Atlantic context and global ice volume changes. In addition, we discuss the potential atmospheric and oceanic configurations behind this complexity of millennial-scale climate variability during MIS 11.

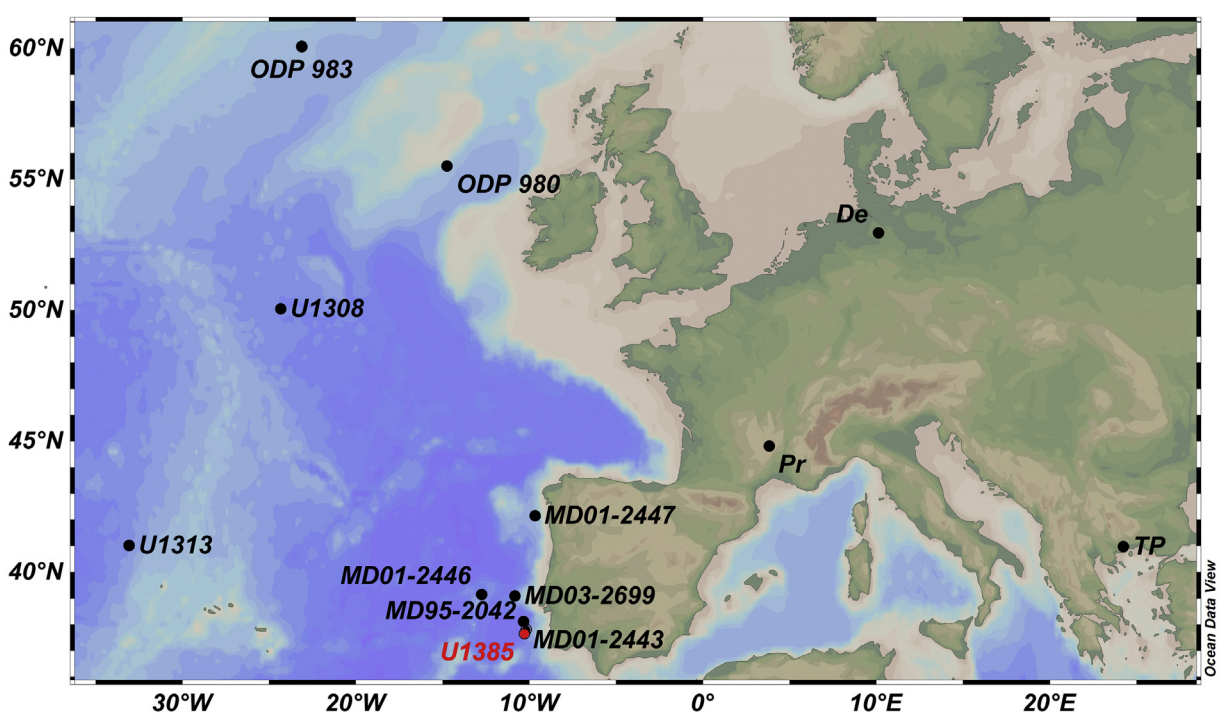

Figure 1. Location of the IODP Site U1385 and available European and North Atlantic records discussed in the text: ODP Site 983 (Barker et al., 2015); ODP Site 980 (Oppo et al., 1998; McManus et al., 1999); De: Dethlingen (Koutsodendris et al., 2010); Site U1308 (Hodell et al., 2008); Pr: Praclaux (Reille et al., 2000); MD01-2447 (Desprat et al., 2005); Site U1313 (Stein et al., 2009); TP: Tenaghi Philippon (Wijmstra and Smit, 1976); MD01-2446 (Voelker et al., 2010; Marino et al., 2014); MD03-2699 (Voelker et al., 2010; Rodrigues et al., 2011; Amore et al., 2012; Palumbo et al., 2013); MD95-2042 (Sánchez Goñi et al., 1999, 2002; Shackleton et al., 2000; Chabaud et al., 2014); MD01-2443 (de Abreu et al., 2005; Martrat et al., 2007; Tzedakis et al., 2009).

Please cite this article in press as: Oliveira, D., et al., The complexity of millennial-scale variability in southwestern Europe during MIS 11, Quaternary Research (2016), http://dx.doi.org/10.1016/j.yqres.2016.09.002

Environmental setting and pollen signal

Site U1385 (Fig. 1) is located on the SW Iberian margin (37°34.285′N, 10°7.562′W; 2578 m below sea level). The modern sea surface circulation of this region is dominated by the Portugal Current System, the descending branch of the eastern North Atlantic subtropical gyre (Fiúza, 1983; Peliz et al., 2005). In spring and summer seasons, the southward-flowing Portugal Current (PC) and subsequent coastal upwelling are induced by strong northerly winds, while in winter the northward warm and saltier surface Iberian Poleward Current (IPC) prevails (Fiúza et al., 1982; Peliz et al., 2005).

The present-day SW Iberian climate is Mediterranean, marked by a pronounced seasonality between warm/dry summers and cool/wet winters, with strong influence of moisture from the Atlantic in the westernmost area (Peinado Lorca and Martinez-Parras, 1987; Gimeno et al., 2010). The North Atlantic Oscillation (NAO) is the major atmospheric pattern dictating winter precipitation variability over western Iberia through changes in the position of the North Atlantic jet stream and storm tracks (e.g., Hurrell, 1995; Trigo et al., 2004). Conversely, summer dryness is tied to the northeastward expansion of the Azores subtropical High, associated with the descending branch of the Hadley cell (Lionello et al., 2006).

The Mediterranean vegetation dominates the Tagus watershed landscape, although its composition varies over the basin (Peinado Lorca and Martínez-Parras, 1987; Blanco Castro et al., 1997). At low altitudes, *Quercus rotundifolia* and *Quercus suber* woodlands with evergreen shrubs *Phillyrea angustifolia* and *Pistacia terebinthus* are the main forest components in the western part of the basin, while evergreen oak woodlands (*Quercus rotundifolia* and *Quercus coccifera*) associated with juniper (*Juniperus communis*) and aleppo pine (*Pinus halepensis*) develop in the eastern part due to decreased maritime influence. In the warmest areas, scattered sclerophyllous trees and shrubs, such as mastic (*Pistacia lentiscus*) and olive (*Olea europea*) are present. In the Iberian mountains, orogenic precipitation and an altitudinal thermal gradient promote the dominance of deciduous oak (*Quercus pyrenaica* and *Quercus faginea*) woodlands at middle altitudes, and pinewoods (*Pinus sylvestris*, *Pinus nigra*) with juniper at higher altitudes. Heathers (Ericaceae) develop in zones with relatively high humidity due to Atlantic influence while evergreen aromatic shrubs (Cistaceae) are found in drier environments (Peinado Lorca and Martínez-Parras, 1987).

Marine sites located near regions with large drainage basins, such as Site U1385, mainly receive pollen grains supplied by rivers (Heusser and Balsam, 1977; Dupont and Wyputta, 2003). Pollen settles down through the water column and ultimately the deep-sea floor, thanks to physical processes such as flocculation, agglomeration and incorporation in fecal pellets (Mudie and McCarthy, 2006). In particular, the Tagus and, to a lesser extent, Sado fluvial systems are the primary pollen suppliers to the deep sea off SW Iberia, thus providing a reliable integrated image of the vegetation from the SW Iberian Peninsula (Naughton et al., 2007).

Material and methods

IODP Site U1385

Site U1385 (Fig. 1) was drilled on the spur Promontorio dos Principes de Avis on the continental slope of the SW Iberian margin (Fig. 1) during the IODP Expedition 339 ("Mediterranean Outflow") on board the D/V JOIDES Resolution (Expedition 339 Scientists, 2013; Hodell et al., 2013b). Four holes (A–E) were cored and accurately correlated on the basis of XRF analyses to construct a composite depth scale (Hodell et al., 2015). This depth scale corrects for distortion in individual cores and is given in corrected revised meters composite depth (crmcd) (Hodell et al., 2015). The sediments are composed of relatively homogeneous hemipelagic mudstones and claystones with different proportions of biogenic carbonate and terrigenous sediment (Expedition 339 Scientists, 2013).

Pollen analysis

Holes E and D were sampled for pollen analysis every 4 cm between 50.27 and 56.01 crmcd and every 2 cm between 54.50 and 56.01 crmcd. The pollen sample preparation technique followed standard palynological procedure employed for marine samples at UMR EPOC, University of Bordeaux, including coarse-sieving (150-μm mesh) and successive chemical treatments (cold 10%, 25% and 50% HCl; cold 45% and 70% HF; cold HCl at 25%). The obtained residue was sieved through 10-μm nylon mesh screens and mounted unstained in glycerol (Desprat, 2005).

Pollen analysis was performed on 170 samples using a Nikon light microscope at ×500 and ×1000 (oil immersion) magnifications. A total of 100–166 pollen grains without *Pinus* were counted in a total pollen sum ranging between 150 and 719 per sample. Twenty to thirty-three different morphotypes were identified in each pollen sample analyzed to ensure a reliable representation of the vegetation community (McAndrew and King, 1976). Identifications followed Moore et al. (1991) and Reille (1992). Pollen data were expressed as percentages of the main sum, which excludes the over-represented *Pinus* (Heusser and Balsam, 1977; Naughton et al., 2007), aquatic plant, indeterminable pollen grains and Pteridophyta spores. *Cedrus* pollen was also excluded from the main sum because it likely originates from North African montane cedar forest (Sánchez Goñi et al., 1999; Magri et al., 2012; Chabaud et al., 2014). *Pinus* and *Cedrus* percentages were calculated using the main sum plus their individual counts. Spore and aquatic percentages were estimated using the total sum (pollen + spores + indeterminable + unknowns).

Pollen percentages were plotted against depth by using the software Psimpoll (Bennett, 2000) (Fig. 2). Pollen zones were established by visual inspection based on fluctuations of at least two ecologically different morphotypes (Birks and Birks, 1980), and statistically confirmed using constrained hierarchical cluster analysis. Clustering of pollen percentages of morphotypes included in the main sum was performed in R environment v. 3.1.1 (R Core Team, 2014), using the function *chclust* from the R package rioja (Juggins, 2009). All temperate tree and shrub taxa excluding *Pinus*, *Cedrus* and Cupressaceae (*Acer*, *Alnus*, *Betula*, *Carpinus*, *Corylus*, *Fagus*, *Fraxinus excelsior*-type, *Hedera helix*, *Ilex*, *Juglans*, *Ligustrum*-type, *Myrica*, *Populus*, *Pterocarya*, *Quercus deciduous*-type, *Rhus*-type, *Salix*, *Tilia*, *Ulex*-type, *Ulmus* and *Vitis*) and Mediterranean taxa (*Cistus*, *Fraxinus ornus*-type, *Olea*, *Phillyrea*, *Pistacia*, *Quercus evergreen*-type and *Quercus suber*-type), were included in the Mediterranean forest (MF) group (Fig. 2), following previous studies off southern Iberia (e.g., Fletcher and Sánchez Goñi, 2008; Sánchez Goñi et al., 2008, 2009, 2013; Chabaud et al., 2014).

A generalized additive mixed model (GAMM) that incorporates temporal correlation was applied to the percentages of the MF group in order to identify rapid forest decline events (Supplementary Fig. S1). We used the *gamm* function from the *mgcv* R package (Wood, 2006; Zuur et al., 2009) to fit a smoothing curve through the data and remove low-frequency variations. Millennial-scale forest decline events were determined based on the two-fold condition that model residuals of at least one sample exceeded one standard deviation (1σ) and that substantial declines in MF

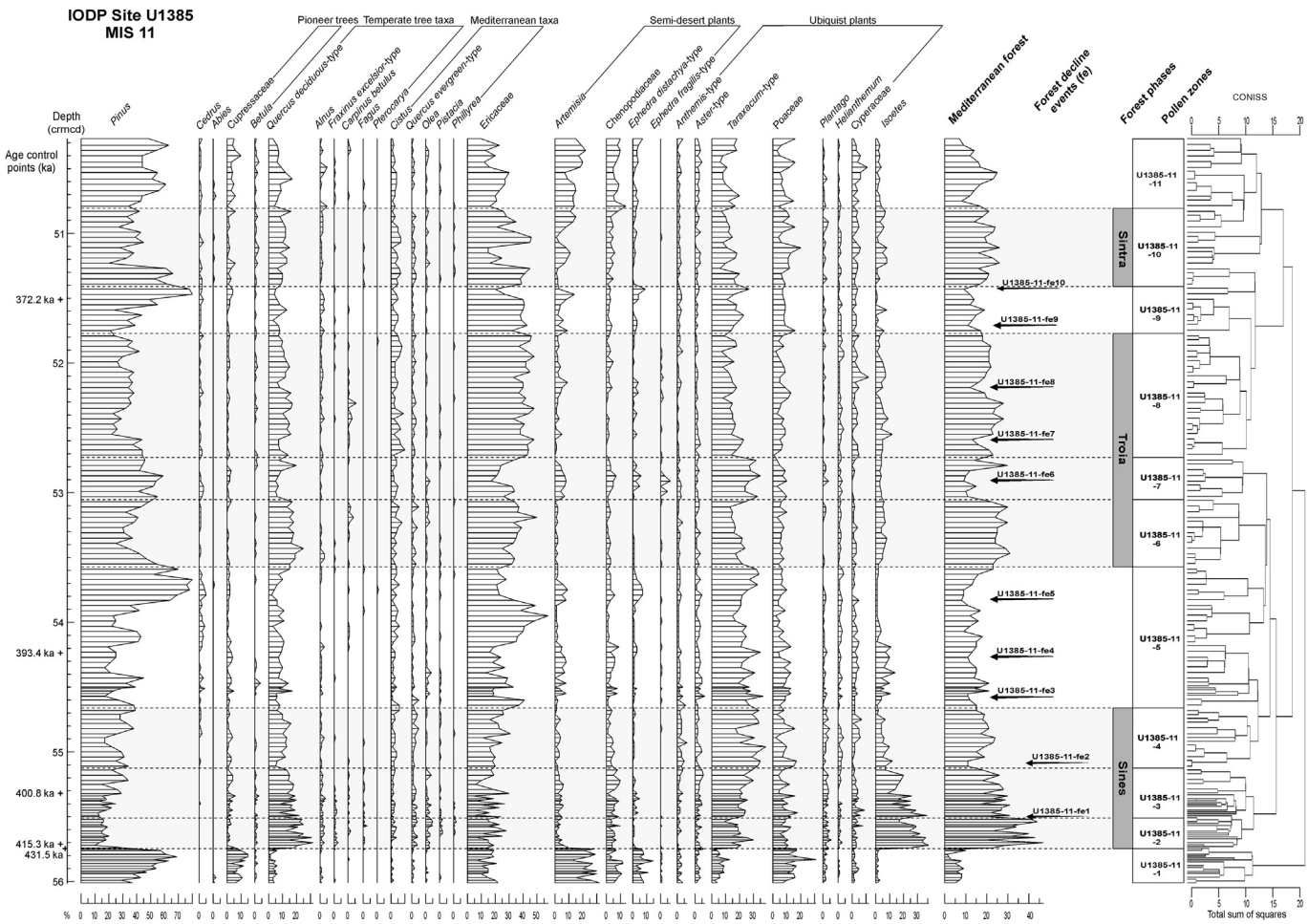

Figure 2. Pollen percentage diagram of selected morphotypes and Mediterranean forest (MF) group at Site U1385 versus depth (crmcd: corrected revised meter composite depth). Position of the control points are indicated with crosses on the left side. MF is composed of all arboreal pollen taxa, mainly deciduous *Quercus* plus Mediterranean taxa, excluding *Pinus*, *Cedrus* and Cupressaceae. Pollen zones and dendrogram showing the results from the hierarchical clustering analysis are represented on the right. Shaded areas indicate forest phases labeled with local names. Arrows underline forest decline events defined using residuals from the GAMM analysis (Supplementary Fig. S1). Pollen zone and event names are designated as following: Site U1385 (site name) and MIS 11 (Marine Isotopic Stage) – followed by the number of the pollen zone and "fe" for forest decline event plus the number of the event, respectively.

percentages (>10%) occur within at least two consecutive samples (Supplementary Fig. S1).

Analysis of marine climatic indicators

Biomarker analyses were carried out in 163 levels from holes E and D, most of them coinciding with pollen analysis levels, at intervals of 1, 2, 4 or 6 cm between 50.29 and 56.02 crmcd. Analyses were performed following the analytical procedure described in Villanueva et al. (1997a). Organic compounds were extracted from sediments and separated using organic solvents, then identified using Bruker Mass spectrometer detector and quantified with Varian Gas chromatograph Model 3800 equipped with a septum programmable injector and a flame ionization detector with a CPSIL-5 CB column. Alkenones concentrations were determined using *n*-hexatriacontane as an internal standard. Alkenone-derived sea surface temperature (Uk'_{37} – SST) was based on the $C_{37:2}$ and $C_{37:3}$ ratio following the global core top calibration (Müller et al., 1998), while the $C_{37:4}$ concentration was used as an indicator for subpolar water influence induced by iceberg melting (Villanueva et al., 1997b; Bard et al., 2000; Martrat et al., 2004, 2007; Rodrigues et al., 2011).

MIS 11 benthic foraminiferal oxygen isotope ($\delta^{18}O_b$) record includes a total of 46 samples between 50.29 and 56.14 crmcd (sampling interval ranging between 1 and 20 cm). It combines the Hodell et al. (2015) dataset and fourteen new levels analyzed to increase the MIS 11c resolution.

Results and interpretations

Chronology

In the light of the new $\delta^{18}O_b$ data, we modified the original chronology from Hodell et al. (2015) for the MIS 12/11 section by using two new control points for correlating the Site U1385 $\delta^{18}O_b$ record to the LR04 benthic stack, which has an uncertainty of ±4 ka (Lisiecki and Raymo, 2005) (Fig. 3, Table 1). Age–depth modeling was based on linear interpolation.

The new $\delta^{18}O_b$ data confirmed the very low sediment rate (0.24 cm/ka) between ~431 and 415 ka (Table 1), which possibly reflects a condensed section or a hiatus between Termination V and early MIS 11c (Hodell et al., 2015). The sedimentation rate increases up to 2.7 cm/ka between ~415 and 401 ka (Table 1), and after the end of MIS 11 $\delta^{18}O_b$ plateau at ~401 ka (Fig. 3) the high

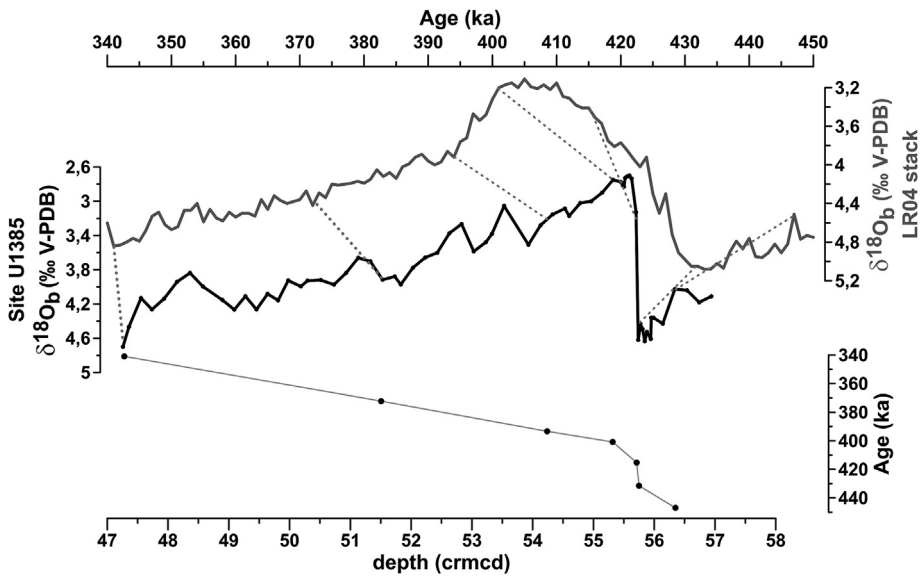

Figure 3. Age model based on the correlation of Site U1385 $\delta^{18}O_b$ record (black line; in depth scale, crmcd: corrected revised meter composite depth) with the LR04 $\delta^{18}O_b$ stack (gray line; in age scale) of Lisiecki and Raymo (2005). Control points used for the correlation between records are depicted with dashed lines. The age–depth model is presented on the bottom.

Table 1
Age control points used to correlate the Site U1385 $\delta^{18}O_b$ record to the LR04 benthic stack of Lisiecki and Raymo (2005) (Hodell et al., 2015); crmcd: corrected revised meter composite depth.

Site U1385 depth (crmcd)	Control points LR04 age (ka)	Sed. Rate (cm/ka)
47.280	340.95	
51.506	372.21	13.52
54.238[a]	393.35[a]	12.92
55.317	400.84	14.41
55.711	415.27	2.73
55.750[a]	431.53[a]	0.24
56.349	446.99	3.87

[a] New control points used in this study.

sedimentation rates and sampling interval allows for a mean time resolution of ~290 yr between pollen samples.

We followed the recent nomenclature recommendation dividing MIS 11 into three substages 11c, 11b and 11a (Railsback et al., 2015) (Fig. 4). However, we also used the decimal event notation of Bassinot et al. (1994) that distinguishes additional isotopic events reflecting orbital-scale variability within MIS 11b. In this context, MIS 11c and MIS 11a encompasses the light isotopic events 11.3 and 11.1, respectively, while MIS 11b incorporates two heavy isotopic events, 11.24 and 11.22, separated by the light isotopic event 11.23 (double peak) (Fig. 4).

Pollen-derived vegetation reconstruction

Pollen analysis results are displayed in a synthetic pollen percentage diagram (Fig. 2) together with a summary of the main features of the pollen zones in Table 2.

Long-term vegetation trends

The pollen record was divided into eleven pollen zones, generally corresponding to the major shifts between forested and open vegetation intervals (Fig. 2), as summarized in Table 2. The forest phases, named Sines, Troia and Sintra, associated with the light isotopic events MIS 11.3, 11.23 and 11.1, respectively, are characterized by an expansion of the Mediterranean forest (MF) mainly composed of deciduous oak and Mediterranean taxa (Figs. 2 and 4). MF percentages range between ~20 and 50%, indicating atmospheric warmth and moisture availability in SW Iberia (Figs. 2 and 4).

Sines is the longest, warmest and most floristically diverse forest phase documented in our record (Figs. 2 and 4). Sines duration is about 26 ka, although chronological uncertainties during Termination V preclude the precise identification of its onset. The optimal expression of the Mediterranean climate, i.e. warmest conditions with highly seasonal rainfall, is suggested by the highest abundances of Mediterranean taxa between ~414 and 408 ka (Fig. 4). This warmest phase was followed by a progressive contraction of MF and expansion of dry-grasslands (mostly Poaceae, Asteraceae and semi-desert plants, i.e. *Artemisia*, Chenopodiaceae and both *Ephedra* types, as defined by Polunin and Walters (1985)), indicating cooler and drier conditions over the end of Sines forest phase (Figs. 2 and 4). During the second forest phase, Troia (~13.9 ka), deciduous *Quercus* woodland with heathland (Ericaceae) dominated the landscape (Figs. 2 and 4), reflecting more humid and temperate conditions than during Sines interglacial. The MF moderately expanded during the last forest phase, Sintra (~4.4 ka), suggesting a weaker increase in warmth and moisture availability (Figs. 2 and 4).

Open vegetation phases, encompassing the heavy isotopic events 11.24 and 11.22 (Fig. 4), ~396.5 to 388.5 ka and from ~374.5 to 371.5 ka, are represented by MF values below 20%, in accordance with studies on modern samples (e.g., Wright et al., 1967; Prentice, 1978; Petersen, 1983). Such change suggests a shift towards cooler and drier conditions since temperature, and particularly moisture availability, are critical for forest composition and development in the Mediterranean region (Quezel, 2002). Both open vegetation phases are characterized by alternations between dominance of heathland and dry-grassland (Figs. 2 and 4). The progressive replacement of MF by Ericaceae likely reflects cooling with sustained humidity year-round, although heath requires less water than forest (Walter and Breckle, 1989; Loidi et al., 2007). In contrast, dry-grassland expansion indicates cold and more pronounced dry conditions, with semi-desert plants being an indicator of lower moisture availability than Poaceae–Asteraceae (Polunin and

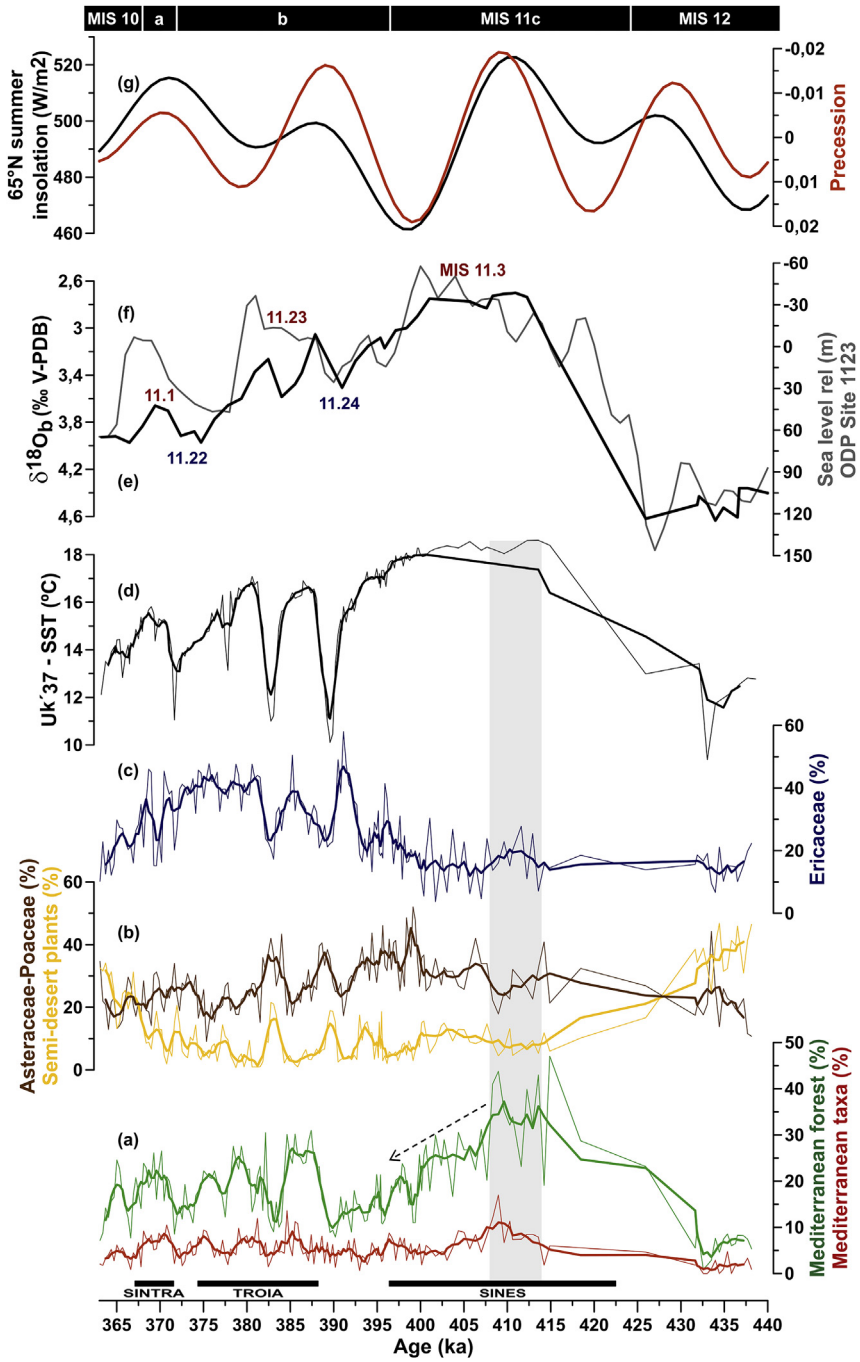

Figure 4. MIS 11 long-term vegetation and climatic changes at Site U1385. From the bottom to the top: Percentages of selected pollen taxa or group of taxa: (a) Mediterranean taxa (*Quercus evergreen*-type, *Quercus suber*-type, *Cistus*, *Olea*, *Phillyrea*, *Pistacia and Fraxinus ornus*-type) (red line) and Mediterranean forest (MF, all arboreal pollen taxa, mainly deciduous *Quercus* plus Mediterranean taxa, excluding *Pinus*, *Cedrus* and Cupressaceae) (green line), (b) semi-desert plants (*Artemisia*, Chenopodiaceae, *Ephedra distachya*-type and *Ephedra fragilis*-type) (yellow line) and Asteraceae–Poaceae group (brown line), (c) Ericaceae; U1385 marine data: (d) Uk'_{37} – SST and (e) $\delta^{18}O_b$ record (black line) with marine isotope events according to Bassinot et al. (1994); (f) Relative sea level changes (gray line) based on ODP 1123 $\delta^{18}O_{seawater}$ (Elderfield et al., 2012); (g) 65°N summer insolation (black line) and precession index (red line) (Berger, 1978). Forest phases and marine isotopic substages on bottom and top, respectively. Bold lines represent 5-point moving averages of pollen percentages and Uk'_{37} – SST. The gray bar indicates the MF maximal expansion during Sines forest phase. (For interpretation of the references to color in this figure legend, the reader is referred to the web version of this article.)

Walters, 1985). The last open vegetation interval, between ~371.5 and 363 ka, is characterized by the dominance of semi-desert plants, including the substantial expansion of *Ephedra*, suggesting the setting of overall dry and cold glacial conditions during the early stages of MIS 10 (Figs. 2 and 4). This interval also depicts a brief expansion of MF at ~365 ka representing an interstadial-type episode during MIS 10.

Suborbital vegetation dynamics

Superimposed on the long-term vegetation changes, the pollen record at Site U1385 provides evidence for repeated short-term climate variations of different character and intensity throughout MIS 11 in SW Iberia. Nine millennial-scale forest decline events (U1385-11-fe-2 to -fe10) were identified using the twofold

Table 2
Description and interpretation of the MIS 11 pollen record at Site U1385. Mediterranean forest (MF) decline events (fe) are indicated in the last column. Gray shaded bar mark the interval during MIS 12/11 transition to early MIS 11 with anomalous low sedimentation rate probably corresponding to a condensed section or hiatus (Hodell et al., 2015).

Forest phases	Pollen zones (basal depth in crmcd; age in ka)	Duration of intervals (ka) (number of samples)	Pollen signature	Forest decline events (fe)
	U1385-11-11 (50.83; 367.2)	≥4 (13)	Marked drop of Mediterranean forest (MF), Ericaceae and *Isoetes* values along with high frequencies of semi-desert plants (in particular *Artemisia*, Chenopodiaceae and *Ephedra distachya*-type), *Pinus* and Cupressaceae. Brief but distinct rise of oak percentages at the middle of the zone while semi-desert plants decrease. Continuous presence of *Cedrus* and occurrences of *Abies*.	
Sintra	**U1385-11-10** (51.43; 371.6)	4.4 (15)	Increase of MF taxa values (mainly deciduous and evergreen *Quercus*, *Cistus*, *Olea* and occurrences of *Pistacia* and *Phillyrea*) and *Isoetes*. High percentages of Ericaceae, but showing a distinct decline by the middle of the zone and a decreasing trend by the top mainly in favor of semi-desert plants. Lower abundances of *Pinus*, *Cedrus*, Cupressaceae and *Taraxacum*-type.	
	U1385-11-9 (51.79; 374.4)	2.8 (9)	Important decline of MF taxa percentages and high representation of semi-desert taxa, *Taraxacum*-type, Poaceae, Cupressaceae, *Cedrus* and *Pinus*. Short-lived increase of deciduous *Quercus* by the middle of the zone coupled with a reduction in semi-desert taxa values. By top of the zone, the second deciduous *Quercus* decrease is simultaneous with the drop of Ericaceae values and higher increase of semi-desert plants.	U1385-11-fe10 U1385-11-fe9
Troia	**U1385-11-8** (52.75; 381.8)	7.4 (24)	Percentages of semi-desert plants, *Taraxacum*-type and *Pinus* decrease while those of Mediterranean taxa returns to higher abundances. Highest Ericaceae values. Rise of Cyperaceae, Poaceae and *Isoetes* followed by a decreasing trend by the end of the zone.	U1385-11-fe8 U1385-11-fe7
	U1385-11-7 (53.07; 384.3)	2.5 (8)	Pronounced decline in MF taxa values and Ericaceae associated with an increase of all semi-desert plants, herbs taxa (mainly *Taraxacum*-type), pioneer trees, *Cedrus* and *Pinus*. *Quercus* deciduous sharp increase at the end of the zone coupled with lower percentages of semi-desert plants and *Pinus*.	U1385-11-fe6
	U1385-11-6 (53.59; 388.3)	4 (13)	Rise of MF taxa values (principally deciduous and evergreen *Quercus*, *Alnus*, *Fraxinus excelsior*-type, *Carpinus betulus* and *Olea*), coinciding with higher percentages of Ericaceae and *Isoetes*, and the fall of ubiquist grasses (mainly *Taraxacum*-type). Low semi-desert plants, pioneer trees and *Cedrus* frequencies. *Pinus* percentages decline in lower part of the zone followed by a rise until the top.	
	U1385-11-5 (54.68; 396.4)	8.1 (30)	Lower abundances of MF taxa (mostly deciduous oak) and higher representation of ubiquist plants (in particular *Taraxacum*-type) and *Cedrus*. Ericaceae is detected in moderate to high abundances, with marked fluctuations in favor of semi-desert plants and/or *Taraxacum*-type. By the end of the zone increasing values of MF associated with maximum *Taraxacum*-type are concomitant with decreasing semi-desert taxa and *Pinus* percentages.	U1385-11-fe5 U1385-11-fe4 U1385-11-fe3
Sines	**U1385-11-4** (55.14; 399.6)	3.2 (13)	Intermediate values of deciduous *Quercus* along with reduced percentages of the other temperate trees and high herbaceous abundances (mainly represented by Asteraceae, Poaceae and Ericaceae). Drop of semi-desert taxa and *Isoetes* frequencies.	U1385-11-fe2
	U1385-11-3 (55.52; 408.3)	8.5 (17)	Fall of deciduous oak frequencies and Mediterranean taxa whereas *Taraxacum*-type and semi-desert taxa increase (in particular Chenopodiaceae and *Ephedra distachya*-type). Rise of Poaceae and *Isoetes* at the beginning followed by a decrease along the zone. Lower and oscillating Ericaceae values. Increasing *Pinus* abundances.	U1385-11-fe1
	U1385-11-2 (55.74; 425.9)	14.2 (12)	Abrupt rise in MF taxa percentages (particularly deciduous and evergreen *Quercus*, *Alnus*, *Fraxinus excelsior*-type, *Cistus* and *Olea*). Pronounced decrease in *Pinus*, Cupressaceae, Poaceae and semi-desert plants values, while *Taraxacum*-type and *Isoetes* increase strongly. Highest Mediterranean taxa abundances at the top of the zone coinciding with Ericaceae, *Taraxacum*-type and *Isoetes* drop.	
MIS 12/11 transition	**U1385-11-1** (56.01; 438.1)	>15.9 (16)	Strong dominance of non-arboreal pollen (NAP) taxa, in particular semi-desert plants, grassland taxa (mainly Poaceae and *Taraxacum*-type) and Ericaceae. Low frequencies of all tree taxa, except Cupressaceae and *Pinus*.	

condition previously described (Figs. 2 and 5 and Supplementary S1). We additionally identified one event (U1385-11-fe1) which displays a substantial decrease in MF of ~20%, although marked by only one data-point. This significant abrupt forest contraction with no recovery suggests the occurrence of a millennial-scale event such as that previously inferred from the SW Iberian margin pollen record within MIS 9e and 7e (Tzedakis et al., 2004). Duration of the MF decline events, defined as the interval between the mid-points of the decline and increase in MF values, varies from ~700 yr (U1385-11-fe2 and fe-7) to ~2100 yr (U1385-11-fe5).

The MF decline events U1385-11-fe1, -fe4, -fe8 and -fe9 (at ~408, 393.5, 377.5 and 373.5 ka, respectively) are characterized by an increase in semi-desert plants of up to ~15%, implying cool and dry conditions (Fig. 5). In addition, the associated herbaceous components vary revealing differences in the degree of moisture deficiency between events: U1385-11-fe1 and -fe4 (highest dry-grassland values) appear drier than U1385-11-fe8 and -fe9 (Fig. 5).

During the forest decline events U1385-11-fe2, -fe3, and -fe7 (centered at ~399.5, 396 and 380.5 ka, respectively), semi-desert plants did not expand (Fig. 5). Asteraceae–Poaceae strongly expanded during U1385-11-fe2 reflecting a weaker shift to cool and dry atmospheric conditions, while Ericaceae dominated over U1385-11-fe3 and -fe7, hence suggesting a cooling with higher annual humidity (Fig. 5).

The most severe forest decline events, U1385-11-fe5, -fe6 and -fe10 (centered at ~390, 383 and 371.5 ka, respectively), are consistently represented by pronounced expansions of semi-desert elements (~20%), minimal MF cover (<10%) and Ericaceae decrease (Fig. 5), suggesting the coldest and driest atmospheric conditions of MIS 11. Interestingly, these events are also associated with high relative abundances of *Cedrus* and *Pinus* (Fig. 5). The few detailed available pollen records suggest that cedar was, however, absent from Iberia throughout the Quaternary (Magri, 2012). Given the current distribution of cedar in cool and moist high altitude habitats of northern Africa (Cheddadi et al., 1998) and its anemophily, peaks in *Cedrus* in the Iberian margin sediments during cold periods likely resulted from enhanced wind-driven pollen supply (Sánchez Goñi et al., 1999; Chabaud et al., 2014). The peaks of pine

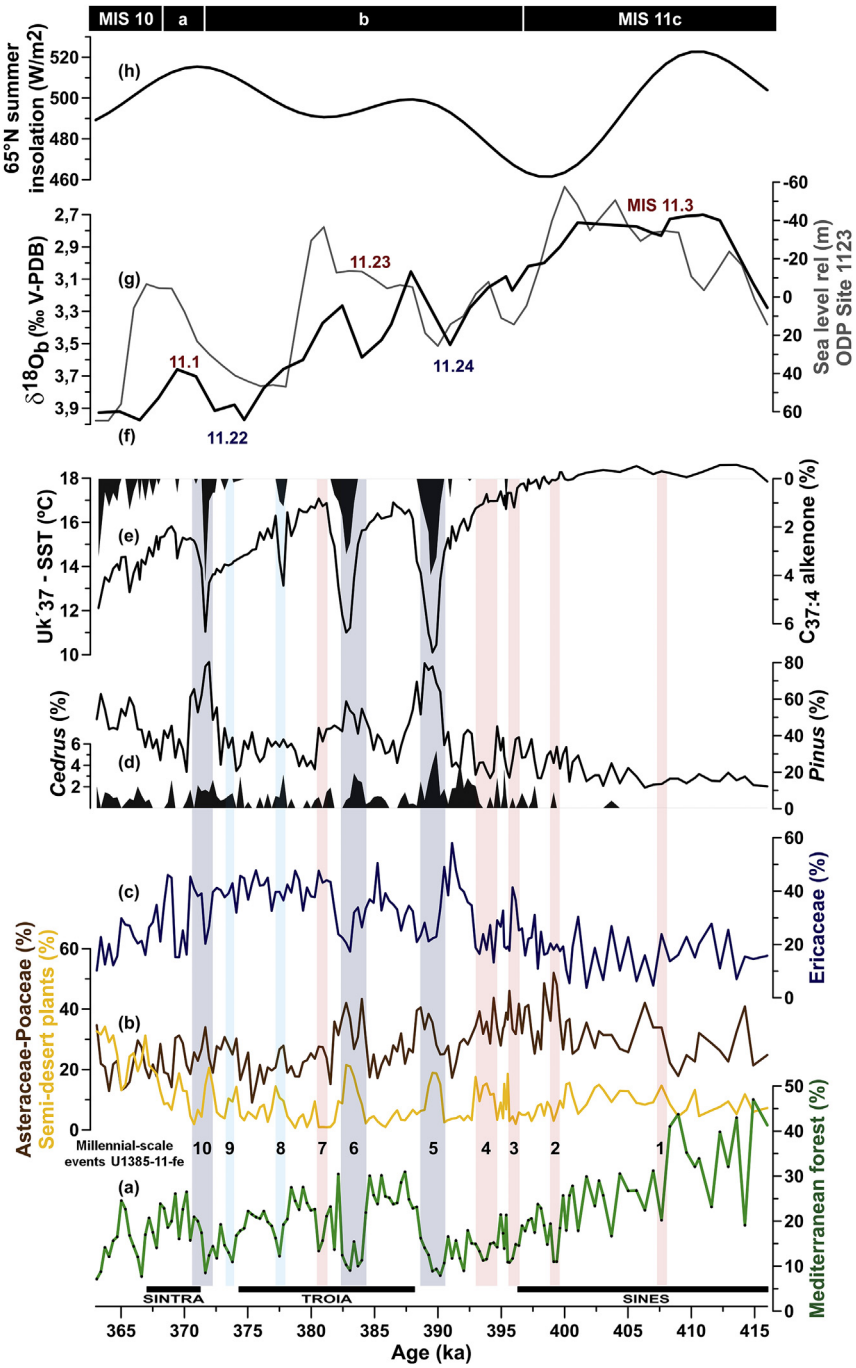

Figure 5. Millennial-scale Mediterranean forest (MF) decline events and oceanic surface changes from Site U1385 direct land-ocean comparison. From the bottom to the top: Selected pollen percentage curves: (a) MF, (b) semi-desert plants (yellow line) and Asteraceae–Poaceae group (brown line), (c) Ericaceae, (d) *Pinus* and *Cedrus*; U1385 marine data: (e) Uk'_{37} – SST and % $C_{37:4}$ – based surface ocean freshwater inputs; (f) $\delta^{18}O_b$ record (black line) with marine isotope events according to Bassinot et al. (1994); (g) Relative sea level changes (gray line) based on ODP 1123 $\delta^{18}O_{seawater}$ (Elderfield et al., 2012); (h) 65°N summer insolation (Berger, 1978). Forest phases and marine isotopic substages on bottom and top, respectively. Numbered blue bands mark the millennial-scale events of high (5, 6 and 10) (dark blue) and moderate (8, 9) (light blue) intensity, while numbered pink bands (1, 2, 3, 4 and 7) represent the MF decline events without counterpart in the SST record. (For interpretation of the references to color in this figure legend, the reader is referred to the web version of this article.)

pollen remain difficult to interpret due to the low taxonomical resolution of the *Pinus* morphotype including pollen from Iberian highland and Mediterranean pine species (Desprat el al., 2015). However, since pine pollen is wind-pollinated and highly buoyant in the air (Birks and Birks, 1980), *Pinus* peaks in the SW Iberian margin during cold events may also result from high intensity winds. These cold, dry and windy events are also noticeably long with a duration between ~1600 and 2100 yr.

Alkenone–sea surface temperature reconstruction

The Uk'_{37} – SST at Site U1385 describe an increasing SST profile from ~9°C to 18°C during Termination V (Fig. 4). Nevertheless, the low sedimentation rates and chronological uncertainties hinder the identification of sea surface water variability during this interval. SSTs remained warm and relatively stable around 18°C up to ~400 ka. At this time, both SST and $\delta^{18}O_b$ initiated a cooling and

heavier long-term trend towards MIS 10 glacial conditions (Fig. 4). Three prominent cooling episodes with temperatures close to 10°C interrupted this trend at ~390 ka (MIS 11.24), ~383 ka (mid MIS 11.23) and ~372 ka (MIS 11.22) (Fig. 5). These cooling events are associated with the strongest $\%C_{37:4}$ increases suggesting freshwater/iceberg discharges (Fig. 5). In addition, a moderate cooling event with SST decreasing down to ~13°C and a minor increase in $\%C_{37:4}$ is detected at ~378 ka (Fig. 5).

Discussion

Long-term vegetation and climatic changes

The MIS 11 long-term vegetation pattern detected at Site U1385 (Fig. 4) has already been documented for NW and SW Iberia (Desprat et al., 2005; Tzedakis et al., 2009), northwestern Greece (Wijmstra and Smit, 1976; Tzedakis et al., 2001) and southern France (Reille et al., 2000; de Beaulieu et al., 2001).

The close correspondence of Sines, Troia and Sintra major forest expansion with maxima in northern hemisphere (NH) summer insolation and low ice volume intervals (Fig. 4) reflects the influence of orbital-scale climatic variability on SW Iberian vegetation. In line with previous works (Desprat et al., 2005; Tzedakis et al., 2009), our pollen record shows the highest degree of warming in Iberia associated with the strongest NH summer insolation maxima of MIS 11c. The three forest extent maxima observed during Sines, Troia and Sintra do not parallel the magnitude of the three insolation maxima but that of precession minima (Fig. 4). In particular, the largest expansion of mixed oak forest and Mediterranean taxa during Sines, reflecting the warmest and strongest rainfall seasonality, occurred during the strongest MIS 11 precession minimum. However, despite the relatively higher sea level and equivalent CO_2 concentrations during MIS 11c (Dutton et al., 2015), the extent of woodland vegetation remained low in comparison with that of warm stages marked by large precession minima such as MIS 5e (Sánchez Goñi et al., 1999). These observations confirm that precession plays a major role on the forest extent in the Mediterranean region south of 40°N (Sánchez Goñi et al., 2008).

As described for other Iberian margin records (Desprat et al., 2005; Tzedakis et al., 2009), the long-term forest decline during the final phase of MIS 11c, i.e. the end of Sines (~408–396 ka), parallels the decrease in NH summer insolation (Fig. 4). This western Iberian long-term vegetation response to insolation forcing is similar to other interglacial periods of the last 400 ka (Tzedakis et al., 2004; Sánchez Goñi et al., 2005; Roucoux et al., 2006; Desprat et al., 2007, 2009; Naughton et al., 2007; Chabaud et al., 2014). However, while conditions on land progressively cooled during late MIS 11c, SSTs remained relatively warm, experiencing solely a subtle decrease from ~18.5°C to 17.5°C (Fig. 4). Pervasive relatively warm conditions off SW Iberia may reflect the persistent dominance of the subtropical Azores Current (AzC) and Iberian Poleward Current (IPC) in this area over the final phase of MIS 11c (Voelker et al., 2010), even after the onset of the NH ice sheet growth at ~400 ka (Fig. 4).

Millennial-scale climate variability

The outstanding features of the multiproxy record at Site U1385 are the pervasive millennial-scale climate instabilities throughout MIS 11 and their diversity as depicted by different regional vegetation and eastern North Atlantic SST changes (Figs. 5 and 6).

Intra-interglacial climate variability during MIS 11c ice volume minimum

The intriguing abrupt MF contraction recorded within MIS 11c at ~408 ka (Fig. 5), event U1385-11-fe1, is also detected within age uncertainties in the closest MD01-2443 pollen record at ~406 ka (Tzedakis et al., 2009). Similarly to Site U1385, this event occurred well before the end of the benthic $\delta^{18}O_b$ plateau and the forest did not recover afterwards. However, this high-amplitude MF change does not have a counterpart either in the SST profile from core MD01-2443 or in other records from the mid-latitude North Atlantic, which consistently report a single cooling event at ~412 ka separating the two MIS 11c warm SST plateaus (Martrat et al., 2007; Stein et al., 2009; Voelker et al., 2010; Rodrigues et al., 2011). This short-term cooling, also observed in the MD01-2443 pollen record (Tzedakis et al., 2009), probably corresponds to the pronounced MF decrease identified at Site U1385 at ~411.6 ka (Figs. 5 and 6 and Supplementary S1). Nevertheless, the very low sedimentation rate of Site U1385 during early MIS 11c prevents further discussion about this specific millennial-scale event.

Intra-interglacial vegetation and climate changes during MIS 11c were also detected in northern Europe. In particular, the Dethlingen varved pollen sequence displays an abrupt cooling event during the Holsteinian interglacial named "Older Holsteinian Oscillation" (OHO) (Koutsodendris et al., 2010, 2011, 2012). Although the timing of the OHO is still debated (Koutsodendris et al., 2012; Tye et al., 2016), Koutsodendris et al. (2012) argued that it most probably occurred at ~408 (±0.5) ka based on the assumption that Holsteinian interglacial correlates with the later part of MIS 11c (~415–397 ka), coinciding with the NH summer insolation maximum, low global ice volume, and highest temperatures in the North Atlantic and Antarctica. Relying on this assumption, the U1385-11-fe1 event, which after our chronology is also detected at ~408 ka, would correspond to the OHO widely recognized in pollen records from the British Islands to Poland north of 50° latitude (Koutsodendris et al., 2012 and references therein). However, the impact of this abrupt climatic oscillation on the vegetation of northern Europe strongly differed from that of SW Iberia. In contrast to SW Iberia (Tzedakis et al., 2009; this study), the northern European forest recovered after the rapid climate change. Comparison of the OHO duration (~300 yr) and its equivalent events in SW Iberia is prevented by the lower time resolution of the pollen records at Site U1385 and MD01-2443 (Tzedakis et al., 2009).

Koutsodendris et al. (2012) additionally proposed that the OHO is analogous to the early Holocene 8.2 ka event in respect with terrestrial ecosystem changes, boundary conditions (reduced NH ice sheets and high NH summer insolation) and European spatial and climatic patterns. Based on these similarities, the OHO could be triggered by a similar forcing mechanism to the 8.2 ka event (Koutsodendris et al., 2012), i.e. a slowdown of the NADW formation induced by freshwater pulse from proglacial lake discharges (Alley and Ágústsdóttir, 2005). Chronological uncertainties preclude the assessment of the AMOC change at the time of this event (e.g., Oppo et al., 1998). The vegetation changes associated with the U1385-11-fe1 event and the 8.2 ka event recorded in the Iberian margin twin cores U1385 and MD95-2042 (Chabaud et al., 2014) support the hypothesis of an analogous terrestrial response to the intra-interglacial events. They are both associated with a rapid and high-amplitude MF contraction that marked the end of the maximum forest expansion, after which the MF did not recover.

However, the analogy between both events is hampered when comparing Iberian SST patterns. While no corresponding sea surface cooling event is detected on the Iberian margin during

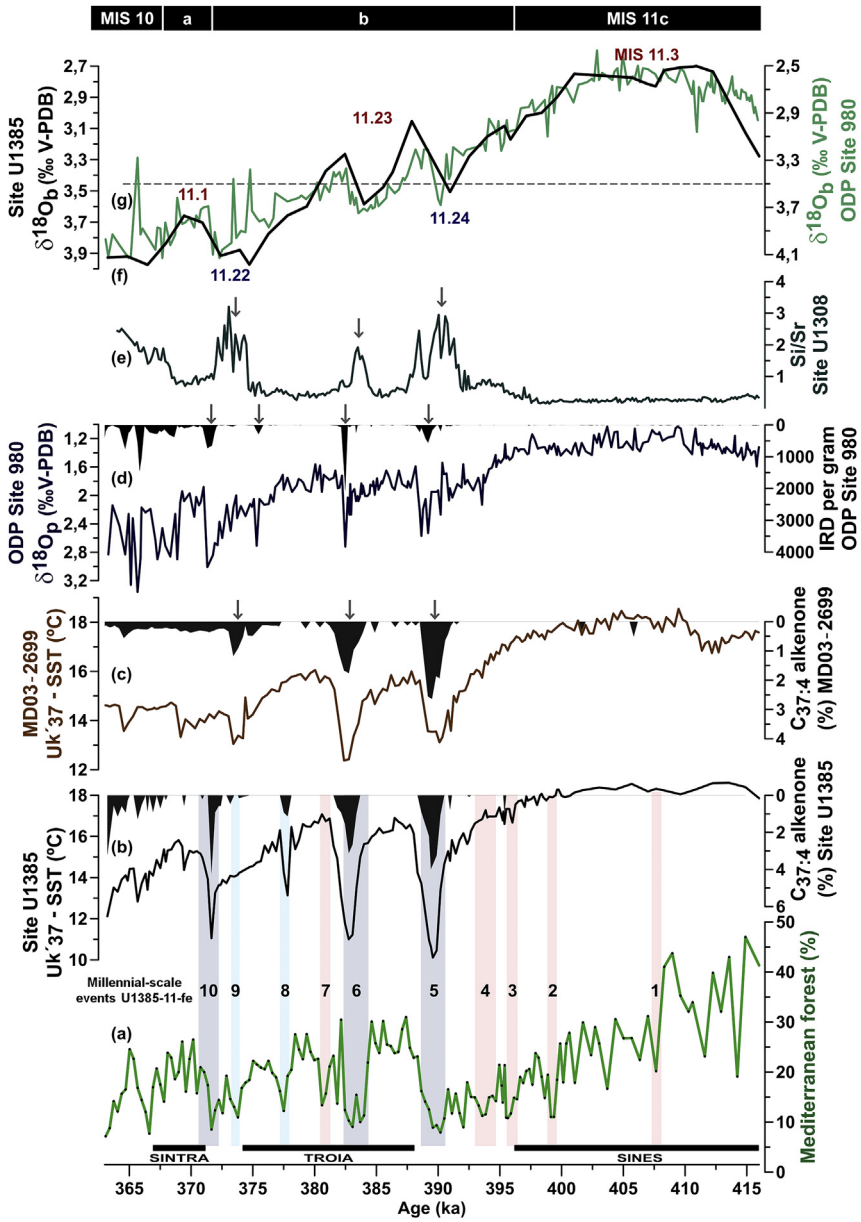

Figure 6. Millennial-scale variability derived from Site U1385 direct land-ocean comparison. (a) Pollen percentage curve of the Mediterranean forest (MF) and (b) Uk'_{37} − SST and % $C_{37:4}$ − based surface ocean freshwater inputs, in comparison with (c) Uk'_{37} − SST and % $C_{37:4}$ from Iberian margin core MD03-2699 (Voelker et al., 2010; Rodrigues et al., 2011), (d) planktic $\delta^{18}O$ and ice rafted detritus (IRD) concentrations (grains/g) at ODP 980 (Oppo et al., 1998) on its LR04 chronology (Lisiecki and Raymo, 2005), and (e) Si/Sr ratio from Site U1308 (Hodell et al., 2008). $\delta^{18}O_b$ records at Sites (f) U1385 (black line) and (g) ODP 980 (green line) with marine isotope events according to Bassinot et al. (1994). Dashed line designates the ice volume threshold of McManus et al. (1999). Forest phases and marine isotopic substages on bottom and top, respectively. Numbered blue bands mark the millennial-scale events of high (5, 6 and 10) (dark blue) and moderate (8, 9) (light blue) intensity, while numbered pink bands (1, 2, 3, 4 and 7) represent the MF decline events without counterpart in the SST record. (For interpretation of the references to color in this figure legend, the reader is referred to the web version of this article.)

the warmest interval of MIS 11c (Martrat et al., 2007; Voelker et al., 2010; Rodrigues et al., 2011), one is observed during the 8.2 ka event (Rodrigues et al., 2009). Additionally, whereas the 8.2 ka event occurred during the retreat of substantial NH ice sheets, the MIS 11 intra-interglacial event might have occurred after the complete melting of the NH continental ice sheets and consequently not as a result of deglacial processes. As recently argued by Raymo and Mitrovica (2012), MIS 11 sea-level highstand, which occurred from 410 to 401 ka, was higher than at present-day, probably resulting from the Greenland Ice Sheet (GIS) and West Antarctic Ice Sheet collapse. Moreover, while the southern GIS persisted through the Holocene (Colville et al., 2011), a nearly ice-free Greenland regime, which promoted the regional development of boreal coniferous forest (de Vernal and Hillaire-Marcel, 2008), likely characterized the late MIS 11c (Reyes et al., 2014). Therefore, the U1385-11-fe1 may be more alike to the mid- to late Holocene events that occurred during minimum NH ice sheets (Combourieu-Nebout et al., 2009; Desprat et al., 2013). Because the MF development is controlled by the wintertime conditions, especially by precipitation (Quezel, 2002; Gouveia et al., 2008), forest contractions without concomitant SST reversals, as observed during U1385-11-fe1, are likely related to a moisture deficiency. Millennial-scale oscillations of the zonal flow recalling the present-day atmospheric patterns tightly linked to blocking episodes in the

North Atlantic (NAO) and Europe (Scandinavian pattern) (Sousa et al., 2015b) appear therefore as a cause of this type of forest declines mainly driven by increased dryness. In fact, for the last millennia, atmospheric centennial variability related to NAO-type events was observed despite the small changes in SST (Moffa-Sanchéz et al., 2014; Ortega et al., 2015). NAO-type circulation possibly driven by an internal oscillation in interglacial AMOC strength was also involved in explaining western Mediterranean multi-centennial climate variability of the mid- to late Holocene (Fletcher et al., 2012). The enhanced dryness associated with U1385-11-fe1 event supports a shift to more persistent positive mode of the NAO-type and, therefore, a weaker influence of the winter mid-latitude North Atlantic westerlies in the SW Iberia.

Decoupled atmospheric and oceanic changes during the glacial inception

The MIS 11c/11 b transition and the late part of MIS 11.23, both characterized by weak ice sheet growth, were punctuated by millennial-scale cooling and drying events on land, U1385-11-fe2 to -fe4 and fe7 (at ~399.5, 396, 393.5 and ~381 ka, respectively). None of these events has a counterpart in the SST record at Site U1385; they are all associated with warm SSTs, between ~18°C and 16.5°C on the margin (Figs. 5 and 6). These observations are also reflected by nearby MD01-2443 paleoclimatic records (Martrat et al., 2007; Tzedakis et al., 2009) and suggest an air–sea thermal contrast at millennial time scales. The atmospheric processes behind this thermal contrast can be related to a persistent positive mode of NAO-type circulation enhancing dryness in Iberia but impacting weakly local SSTs because of the prevailing influence of subtropical AzC and IPC waters over this time interval (Voelker et al., 2010). The influence of the atmosphere on SST is relatively weak at the local scale due to the large heat capacity of the ocean and very effective heat transport via ocean currents (Oort et al., 1976). Additionally, it has been demonstrated that correlation between NAO and SST was not stationary over the last half century (Walter and Graf, 2002).

The MIS 11c/11b glacial inception, marked by three millennial-scale cooling events, is associated with a period of subtle SST cooling in our record, also detected in other mid-latitude North Atlantic records (de Abreu et al., 2005; Martrat et al., 2007; Stein et al., 2009; Voelker et al., 2010; Rodrigues et al., 2011) and in the northern North Atlantic ODP Site 980 by increasing polar foraminifera percentages (Oppo et al., 1998). This progressive cooling across the North Atlantic region may have increased the temperature gradient favoring the recurrence of positive mode of the NAO-type circulation. It would also explain that the millennial-scale Mediterranean forest recovery was progressively less successful in SW Iberia. Decoupling at millennial time scales between air temperatures and SST on the European margins was similarly reported during the ice sheet growth of MIS 5a/4 transition (Sánchez Goñi et al., 2013), and for the past four glacial inceptions (Cortina et al., 2015). This analogy, despite differences in boundary conditions, suggests increased regional moisture that is transported northward through intensified storm tracks, thereby contributing to ice-growth. Such thermal contrasts between cold air and warm sea surface temperatures may have also operated during the MIS 11c/11b transition, at millennial time scales, enhancing northward moisture transport and the glacial inception.

Land–sea cooling during large ice volume conditions

The events U1385-11-fe5, -fe6 and -fe10 (at ~390, 383 and 371.5 ka, respectively), associated with the isotopic events 11.24, mid 11.23 and 11.22, respectively, are characterized in SW Iberia by the coldest and driest atmospheric conditions of MIS 11, high intensity winds and a particularly long duration, between 1600 and 2100 yr (Fig. 5). These high intensity events are synchronous with strong and sudden drops in SSTs down to 10°C and the highest % $C_{37:4}$, suggesting that the site was under the influence of subpolar water. The nearest MIS 11 pollen record shows close similarities regarding the sequence and intensity of these abrupt forest decline events (Tzedakis et al., 2009), where three major forest contractions related with large SST cooling are observed. Despite their low temporal resolution, the NW Iberian margin and southern France pollen records (Reille et al., 2000; Desprat et al., 2005) also reported three main open vegetation periods associated with the MIS 11 coldest conditions. In the North Atlantic, three major millennial-scale cooling events associated with lithic evidence of iceberg discharges (Fig. 6) are commonly detected and have been linked to changes in AMOC (e.g., Oppo et al., 1998; Martrat et al., 2007; Hodell et al., 2008; Voelker et al., 2010; Rodrigues et al., 2011; Barker et al., 2015). Such suborbital variability is even recorded in other regions of the world, such as Siberia (Prokopenko et al., 2010). By analogy to the last glacial cooling events, specifically to Heinrich Events (HE), enhanced aridity over SW Iberia during these MIS 11 events probably resulted from AMOC changes and further intensification and northward displacement of the westerlies (e.g., Sánchez Goñi et al., 2002). These high-intensity events only occurred during the second part of MIS 11 when sea level substantially lowered (Rohling et al., 2009; Elderfield et al., 2012) (Fig. 6). In particular, our direct land–sea comparison at Site U1385 shows that those events only occurred once surpassing the $\delta^{18}O_b$ 3.5‰ threshold (Figs. 5 and 6), in agreement with the critical ice sheet size threshold suggested by McManus et al. (1999). Changes in $\delta^{18}O_b$ are not just driven by ice volume (Skinner and Shackleton, 2005), but this threshold value represents the overall conditions when ice sheets reach a critical size to modify the hydrological cycle, deflect the main atmospheric streams, or produce rafting ice (McManus et al., 1999). This threshold value in the $\delta^{18}O_b$ is tied to the amplification of millennial-scale cooling by feedback mechanisms associated with ice sheet dynamics, and has been supported by numerous MIS 11 records along the Iberian margin (Desprat et al., 2005; de Abreu et al., 2005; Voelker et al., 2010; Rodrigues et al., 2011), as well as elsewhere in the Atlantic Ocean (Poli et al., 2000; Hall and Becker, 2007; Dickson et al., 2008; Stein et al., 2009).

Compared to the Heinrich Stadial (HS) of the last glacial period, the most severe MIS 11 events are marked by weaker MF contractions and moderate semi-desert plant expansion (e.g., Combourieu-Nebout et al., 2002; Sánchez Goñi et al., 2002). However, they present a similar extent of MF than the first and last phases of HS5 and HS4 with an average MF value of 10% (Sánchez Goñi et al., 2000). This percentage of MF suggests that the atmospheric moisture availability and/or temperatures did not reach the critical bioclimatic threshold for major tree decline, although cold and dry conditions prevailed. The less intense dryness during the first and final phases of HS4 and HS5 have been linked to the source of iceberg surges (Sánchez Goñi et al., 2000), and are considered to have been European ice sheets, rather than the Laurentide ice sheet (Grousset et al., 2000). Such IRD source was also proposed for the MIS 11 events (Voelker et al., 2010; Rodrigues et al., 2011). Other sources of iceberg pulses than the Laurentide ice sheet is also supported by XRF data from Site U1308, showing the absence of Ca/Sr peaks but short-lived increases in Si/Sr ratio (Hodell et al., 2008) (Fig. 6). Modeling results using LGM baseline conditions show that depending on its origin, the freshwater flux affects differentially deep-water formation, sea-ice seasonal range and extent and, consequently, the regional response of air temperatures (Roche

et al., 2010). As for HS5 and HS4, the main source of freshwater discharges during MIS 11 cooling events probably played an important role on the vegetation and climatic response in SW Europe. Our MIS 11 direct land–sea comparison confirms therefore that the ice sheet dynamics is a key factor modulating the amplitude of precipitation and temperature reduction in SW Europe at millennial time scales.

Our data additionally show that the coldest and driest episodes, which are associated with iceberg discharges into the North Atlantic, are also particularly long (Figs. 5 and 6). This observation would confirm that besides amplifying the cooling, iceberg discharges may also promote prolonged stadial conditions (Clark et al., 2007; Barker et al., 2015). It is also worthy to note that the Antarctica temperature record displays only three cooling episodes followed by a gradual warming (Jouzel et al., 2007), that likely correlates with the large and long cold episodes recorded in the North Atlantic and SW Europe. The low resolution of the $\delta^{18}O_b$ record from Site U1385 precludes the assessment of the phase relationship between the two hemispheres in response to climate changes. However, it is likely that as for MIS 19 (Tzedakis et al., 2012), the bipolar see–saw became active when ice volume was large enough to produce ice-rafting episodes and most particularly during events of high magnitude and long duration. During MIS 11, the coldest episodes in the North Atlantic appeared generally longer and more humid in SW Iberia and warmer in Antarctica than those punctuating the last glacial. The MIS 11 coldest episodes are, nevertheless, similar to those characterizing MIS 6 when an enhanced hydrological cycle in the North Atlantic may have contributed to disrupt the AMOC despite the lack of iceberg discharges from the Laurentide ice sheet (Margari et al., 2010). This similarity suggests that the freshwater forcing threshold was also modified during the coldest episodes of MIS 11, facilitating their extended duration (Margari et al., 2010).

Besides this, two additional events are detected in our pollen record, U1385-11-fe8 and -fe9 (~377.5 and 374 ka, respectively), both characterized by weaker expansion of semi-desert plants and relatively moderate contraction of forest, reflecting less intense cooling and drying episodes on land (Fig. 5). While event -fe8 is coeval with a moderate SST cooling of ~3.3°C and a small peak in % $C_{37:4}$, event -fe9 does not appear associated with SST and %$C_{37:4}$ changes (Fig. 5). Despite the low temporal resolution, the MD01-2443 pollen record also documents a forest decline event at the transition MIS 11.23/11.22 that may correlate with event -fe8. Most of the North Atlantic records also display a moderate SST cooling event at the MIS 11.23/11.22 transition (de Abreu et al., 2005; Martrat et al., 2007; Tzedakis et al., 2009) with few IRD grains in the subpolar sediments (Oppo et al., 1998; Barker et al., 2015), possibly suggesting a minor iceberg pulse. Event -fe8 could be assimilated to the group of high intensity events mentioned above although the iceberg discharge, if any, appears too moderate to disrupt the AMOC. The weak and short-lived cold episodes on land and in the ocean, as well as the lack of millennial-scale change in Antarctica concomitant with event -fe8, are in line with a still active AMOC. In contrast with event -fe8, no change in the North Atlantic SST appears related with event -fe9, contemporaneous with maximum in ice volume (MIS 11.22). This finding demonstrates that air–sea decoupling may also be a feature of periods with no ice growth, further illustrating the complexity and diversity of millennial-scale climatic variability.

Conclusions

The new high temporal resolution multiproxy study of MIS 11 at Site U1385 documents SW Iberian vegetation and subtropical eastern North Atlantic sea surface changes at orbital and suborbital time scales.

1. At orbital time scales, our reconstruction shows the three classical forest phases of decreasing extent separated by open vegetation conditions (warm/humid–cold periods). The weak precessional forcing of MIS 11 is reflected in the overall low expansion of the Mediterranean forest (MF) and in particular the Mediterranean taxa, although higher forest expansion coincides with precession minima.
2. At millennial time scales, the Site U1385 pollen record reveals ten MF declines events indicating recurring cool and dry atmospheric episodes throughout MIS 11. The direct comparison between vegetation and oceanic changes allows the characterization of different types of millennial-scale events under distinct boundary conditions, highlighting the key role of ice–ocean–atmosphere interactions in the diversity of suborbital coolings:
   - Site U1385 reveals a number of abrupt forest decline events indicating cooler and drier atmospheric conditions with no concurrent SST change. All these events occurred during low ice volume conditions associated with MIS 11c sea-level highstand, and MIS 11c/11b transition and late MIS 11.23, both characterized by weak ice sheet growth. We propose that these events were probably related with a persistent/frequent positive mode of the NAO-type, which led to enhanced aridity in SW Iberia but had a minor or unsystematic impact on local SSTs. The observed air–sea decoupling during MIS 11c/11b transition highlights the potential role of the thermal contrast on suborbital time scales on glacial inception by increasing northward transport of moisture, hence accelerating northern ice sheet growth.
   - Particularly long, coldest, driest and windy events in SW Europe along with large SST cooling punctuated MIS 11b, an interval with larger ice volume conditions. These high intensity events were contemporaneous with the well-known, prominent North Atlantic cooling events associated with iceberg discharges, likely originating from the European ice sheets. Our record supports that dynamics of northern ice sheets was a key factor for amplifying the magnitude of precipitation and temperature reduction in SW Europe and extending the duration of these abrupt climate changes. Modulation of millennial-scale cooling events likely involves positive feedback mechanisms on AMOC related to freshwater from melting icebergs, changes in regional precipitation and the differential impact of iceberg discharges on deep-water circulation and regional climates depending on their origin. In addition, the sequence of these high intensity events correlates with warming in Antarctica suggesting that the interhemispheric link through the bipolar see–saw was active despite the European origin for iceberg pulses.

Acknowledgments

This study used samples provided by the IODP Expedition 339. This work was funded by *WarmClim*, a CNRS LEFE-INSU IMAGO project. This research was also supported by the Portuguese Foundation for Science and Technology (FCT) through the project CLIMHOL (PTDC/AAC-CLI/100157/2008) and D. Oliveira's doctoral grant (SFRH/BD/9079/2012). We are very grateful to L. Devaux for technical assistance, as well as J. Etourneau and Z. Stroynowski for their helpful comments and editing. The editor Derek Booth, Terri Lacourse, Adele Bertini, Ian Candy and anonymous reviewer are thanked for their thoughtful suggestions.

Appendix A. Supplementary data

Supplementary data related to this article can be found at http://dx.doi.org/10.1016/j.yqres.2016.09.002.

References

Alley, R., Ágústsdóttir, A.M., 2005. The 8k event: cause and consequences of a major Holocene abrupt climate change. Quaternary Science Reviews 24, 1123–1149.

Amore, F.O., Flores, J.A., Voelker, A.H.L., Lebreiro, S.M., Palumbo, E., Sierro, F.J., 2012. A middle Pleistocene northeast Atlantic coccolithophore record: paleoclimatology and paleoproductivity aspects. Marine Micropaleontology 90–91, 44–59. http://dx.doi.org/10.1016/j.marmicro.2012.03.006.

Anav, A., Mariotti, A., 2011. Sensitivity of natural vegetation to climate change in the Euro-Mediterranean area. Climate Research 46, 277–292. http://dx.doi.org/10.3354/cr00993.

Bard, E., Rostek, F., Turon, J.L., Gendreau, S., 2000. Hydrological impact of Heinrich events in the subtropical northeast Atlantic. Science 289 (5483), 1321–1324. http://dx.doi.org/10.1126/science.289.5483.1321.

Barker, S., Chen, J., Gong, X., Jonkers, L., Knorr, G., Thornalley, D., 2015. Icebergs not the trigger for North Atlantic cold events. Nature 520, 333–336. http://dx.doi.org/10.1038/nature14330.

Bassinot, F.C., Labeyrie, L.D., Vincent, E., Quidelleur, X., Shackleton, N.J., Lancelot, Y., 1994. The astronomical theory of climate and the age of the Brunhes-Matuyama magnetic reversal. Earth and Planetary Science Letters 126, 91–108.

Bauch, H.A., 2012. Interglacial climates and the Atlantic meridional overturning circulation: is there an Arctic controversy? Quaternary Science Reviews 63, 1–22. http://dx.doi.org/10.1016/j.quascirev.2012.11.023.

Bennett, K.D., 2000. Psimpoll and Pscomb: Computer Programs for Data Plotting and Analysis. Quaternary Geology, Earth Sciences, Uppsala University, Uppsala, Sweden. Software available on the internet at http://www.kv.geo.uu.se.

Berger, A., 1978. Long-term variations of daily insolation and Quaternary climatic changes. Journal of Atmospheric Science 35, 2362–2367.

Billups, K., Chaisson, W., Worsnopp, M., Thunell, R., 2004. Millennial-scale fluctuations in subtropical northwestern Atlantic surface ocean hydrography during the mid-Pleistocene. Paleoceanography 19 (2), PA2017. http://dx.doi.org/10.1029/2003pa000990.

Birks, H., Birks, H., 1980. Quaternary Palaeoecology. Edward Arnold, London.

Blanco Castro, E., Casado González, M.A., Costa Tenori, o M., Escribano Bombín, R., García Antón, M., Génova Fuster, M., Gómez Manzaneque, F., Moreno Sáiz, J.C., Morla Juaristi, C., Regato Pajares, P., Sáiz Ollero, H., 1997. Los bosques ibéricos: una Interpretación Geobotánica. Editorial Planeta, Barcelona, p. 572.

Candy, I., Schreve, D.C., Sherriff, J., Tye, G.J., 2014. Marine Isotope Stage 11: Palaeoclimates, palaeoenvironments and its role as an analogue for the current interglacial. Earth-Science Reviews 128, 18–51. http://dx.doi.org/10.1016/j.earscirev.2013.09.006.

Chabaud, L., Sánchez Goñi, M.F., Desprat, S., Rossignol, L., 2014. Land-sea climatic variability in the eastern North Atlantic subtropical region over the last 14,200 years: atmospheric and oceanic processes at different timescales. The Holocene 24, 787–797. http://dx.doi.org/10.1177/0959683614530439.

Cheddadi, R., Lamb, H.F., Guiot, J., Van Der Kaars, S., 1998. Holocene climatic change in Morocco: a quantitative reconstruction from pollen data. Climate Dynamics 14, 883–890. http://dx.doi.org/10.1007/s003820050262.

Clark, P.U., Hostetler, S.W., Pisias, N.G., Schmittner, A., Meissner, K.J., 2007. Mechanisms for a ~7-kyr climate and sea-level oscillation during Marine Isotope Stage 3. In: Schmittner, A., Chiang, J., Hemming, S. (Eds.), Ocean Circulation: Mechanisms and Impacts. American Geophysical Union, Geophysical Monograph 173, Washington, D.C, pp. 209–246.

Colville, E.J., Carlson, A.E., Beard, B.L., Hatfield, R.G., Stoner, J.S., Reyes, A.V., Ullman, D.J., 2011. Sr-Nd-Pb isotope evidence for ice-sheet presence on southern Greenland during the Last Interglacial. Science 333, 620–623. http://dx.doi.org/10.1126/science.1204673.

Combourieu-Nebout, N., Peyron, O., Dormoy, I., Desprat, S., Beaudouin, C., Kotthoff, U., Marret, F., 2009. Rapid climatic variability in the west Mediterranean during the last 25 000 years from high resolution pollen data. Climate of the Past 5, 503–521. http://dx.doi.org/10.5194/cp-5-503-2009.

Combourieu-Nebout, N., Turon, J.-L., Zahn, R., Capotondi, L., Londeix, L., Pahnke, K., 2002. Enhanced aridity and atmospheric high-pressure stability over the western Mediterranean during the North Atlantic cold events of the past 50 ky. Geology 30, 863–866.

Cortina, A., Sierro, F.J., Flores, J.A., Martrat, B., Grimalt, J.O., 2015. The response of SST to insolation and ice sheet variability from MIS 3 to MIS 11 in the northwestern Mediterranean Sea (Gulf of Lions). Geophysical Research Letters 42, 10,366–10,374. http://dx.doi.org/10.1002/2015GL065539.

de Abreu, L., Abrantes, F., Shackleton, N.J., Tzedakis, P.C., McManus, J.F., Oppo, D.W., Hall, M.A., 2005. Ocean climate variability in the eastern North Atlantic during interglacial Marine Isotope Stage 11: a partial analogue to the Holocene? Paleoceanography 20, 1–15. http://dx.doi.org/10.1029/2004PA001091.

de Beaulieu, J.L., Andrieu-Ponel, V., Reille, M., Grüger, E., Tzedakis, C., Svobodova, H., 2001. An attempt at correlation between the Velay pollen sequence and the Middle Pleistocene stratigraphy from central Europe. Quaternary Science Reviews 20, 1593–1602. http://dx.doi.org/10.1016/S0277-3791(01)00027-0.

de Vernal, A., Hillaire-Marcel, C., 2008. Natural variability of Greenland climate, vegetation, and ice volume during the past million years. Science 320, 1622–1625. http://dx.doi.org/10.1126/science.1153929.

Desprat, S., 2005. Réponses climatiques marines et continentales du Sud-Ouest de l'Europe lors des derniers interglaciaires et des entrées en glaciations. PhD thesis. Bordeaux University, France, 282 pp.

Desprat, S., Combourieu-Nebout, N., Essallami, L., Sicre, M.A., Dormoy, I., Peyron, O., Siani, G., Bout Roumazeilles, V., Turon, J.L., 2013. Deglacial and Holocene vegetation and climatic changes in the southern central Mediterranean from a direct land-sea correlation. Climate of the Past 9, 767–787. http://dx.doi.org/10.5194/cp-9-767-2013.

Desprat, S., Díaz Fernández, P.M., Coulon, T., Ezzat, L., Pessarossi-Langlois, J., Gil, L., Morales-Molino, C., Sánchez Goñi, M.F., 2015. *Pinus nigra* (European black pine) as the dominant species of the last glacial pinewoods in south-western to central Iberia: a morphological study of modern and fossil pollen. Journal of Biogeography 42, 1998–2009. http://dx.doi.org/10.1111/jbi.12566.

Desprat, S., Sanchez Goni, M.F., Naughton, F., Turon, J.-L., Duprat, J., Malaize, B., Cortijo, E., Peypouquet, J.-P., 2007. Climate variability of the last five isotopic interglacials: direct land-sea-ice correlation from the multiproxy analysis of North-Western Iberian margin deep-sea cores. In: Sirocko, F., Litt, T., Claussen, M., Sánchez Goñi, M.F. (Eds.), The Climate of Past Interglacials, Developments in Quaternary Science. Elsevier, pp. 375–386.

Desprat, S., Sánchez Goñi, M.F., McManus, J.F., Duprat, J., Cortijo, E., 2009. Millennial-scale climatic variability between 340000 and 270000 years ago in SW Europe: evidence from a NW Iberian margin pollen sequence. Climate of the Past 5, 53–72. http://dx.doi.org/10.5194/cp-5-53-2009.

Desprat, S., Sánchez Goñi, M.F., Turon, J.L., McManus, J.F., Loutre, M.F., Duprat, J., Malaizé, B., Peyron, O., Peypouquet, J.P., 2005. Is vegetation responsible for glacial inception during periods of muted insolation changes? Quaternary Science Reviews 24, 1361–1374. http://dx.doi.org/10.1016/j.quascirev.2005.01.005.

Dickson, A.J., Leng, M.J., Maslin, M.A., 2008. Mid-depth South Atlantic Ocean circulation and chemical stratification during MIS-10 to 12: implications for atmospheric CO_2. Climate of the Past 4, 333–344. http://dx.doi.org/10.5194/cp-4-333-2008.

Dupont, L.M., Wyputta, U., 2003. Reconstructing pathways of aeolian pollen transport to the marine sediments along the coastline of SW Africa. Quaternary Science Reviews 22, 157–174.

Dutton, A., Carlson, A.E., Long, A.J., Milne, G.A., Clark, P.U., DeConto, R., Horton, B.P., Rahmstorf, S., Raymo, M.E., 2015. Sea-level rise due to polar ice-sheet mass loss during past warm periods. Science 349. http://dx.doi.org/10.1126/science.aaa4019.

Elderfield, H., Ferretti, P., Greaves, M., Crowhurst, S., McCave, N., Hodell, D., Piotrowski, A.M., 2012. Evolution of ocean temperature and ice volume through the Mid- Pleistocene climate transition. Science 377, 704–709. http://dx.doi.org/10.1126/science.1221294.

Expedition 339 Scientists, The Expedition 339 Scientists, 2013. Site U1385. In: Stow, D.A.V., Hernández-Molina, F.J., Alvarez Zarikian, C.A. (Eds.), Proceedings IODP 339. Integrated Ocean Drilling Program Management International, Inc., Tokyo. In: http://dx.doi.org/10.2204/iodp.proc.339.103.201.

Fiúza, A.F.G., 1983. Upwelling patterns off Portugal. In: Suess, E., Thiede, J. (Eds.), Coastal Upwelling, its Sediment Record. Plenum, New York, pp. 85–98.

Fiúza, A.F.G., Macedo, M.E., Guerreiro, M.R., 1982. Climatological space and time variation of the Portuguese coastal upwelling. Oceanologica Acta 5 (1), 31–40.

Fletcher, W.J., Debret, Sánchez Goñi, M.F., 2012. Mid-Holocene emergence of a low-frequency millennial oscillation in western Mediterranean climate: implications for past dynamics of the North Atlantic atmospheric westerlies. The Holocene 23, 153–166. http://dx.doi.org/10.1177/095968361246078.

Fletcher, W.J., Sánchez Goñi, M.F., 2008. Orbital- and sub-orbital-scale climate impacts on vegetation of the western Mediterranean basin over the last 48,000 yr. Quaternary Research 70, 451–464. http://dx.doi.org/10.1016/j.yqres.2008.07.002.

Fletcher, W.J., Sánchez Goñi, M.F., Peyron, O., Dormoy, I., 2010. Abrupt climate changes of the last deglaciation detected in a Western Mediterranean forest record. Climate of the Past 6, 245–264. http://dx.doi.org/10.5194/cp-6-245-2010.

Gao, X., Giorgi, F., 2008. Increased aridity in the Mediterranean region under greenhouse gas forcing estimated from high resolution simulations with a regional climate model. Global and Planetary Change 62, 195–209. http://dx.doi.org/10.1016/j.gloplacha.2008.02.002.

Gouveia, C., Trigo, R.M., DaCamara, C.C., Libonati, R., Pereira, J.M.C., 2008. The North Atlantic oscillation and European vegetation dynamics. International Journal of Climatology 28, 1835–1847.

Gimeno, L., Nieto, R., Trigo, R.M., Vicente-Serrano, S.M., López-Moreno, J.I., 2010. Where does the Iberian Peninsula moisture come From? An answer based on a lagrangian approach. Journal of Hydrometeorology 11, 421–436. http://dx.doi.org/10.1175/2009JHM1182.1.

Giorgi, F., 2006. Climate change hot-spots. Geophysical Research Letters 33, L08707. http://dx.doi.org/10.1029/2006GL025734.

Grousset, F.E., Pujol, C., Labeyrie, L., Auffret, G., Boelaert, A., 2000. Were the North Atlantic Heinrich events triggered by the behavior of the European ice sheets? Geology 28 (2), 123–126.

Hall, I.R., Becker, J., 2007. Deep western boundary current variability in the subtropical northwest Atlantic Ocean during Marine Isotope Stages 12-10. Geochemistry, Geophysics, Geosystems 8, 1–14. http://dx.doi.org/10.1029/2006GC001518.

Heusser, L., Balsam, W.L., 1977. Pollen distribution in the northeast Pacific Ocean. Quaternary Research 7, 45–62. http://dx.doi.org/10.1016/0033-5894(77)90013-8.

Hodell, D., Crowhurst, S., Skinner, L., Tzedakis, P.C., Margari, V., Channell, J.E.T., Kamenov, G., MacLachlan, S., Rothwell, G., 2013a. Response of Iberian Margin sediments to orbital and suborbital forcing over the past 420 ka. Paleoceanography 28, 185–199. http://dx.doi.org/10.1002/palo.20017.

Hodell, D., Lourens, L., Crowhurst, S., Konijnendijk, T., Tjallingii, R., Jimenez-Espejo, F., Skinner, L., Tzedakis, P.C., 2015. A reference time scale for site U1385 (Shackleton site) on the SW Iberian margin. Global and Planetary Change 1385, 49–64. http://dx.doi.org/10.1016/j.gloplacha.2015.07.002.

Hodell, D.A., Channell, J.E.T., Curtis, J.H., Romero, O.E., Röhl, U., 2008. Onset of "Hudson Strait" Heinrich events in the eastern North Atlantic at the end of the middle Pleistocene transition (~640 ka)? Paleoceanography 23, 1–16. http://dx.doi.org/10.1029/2008PA001591.

Hodell, D.A., Lourens, L., Stow, D.V., Hernández-Molina, J., Alvarez Zarikian, C., Shackleton Site Project Members, 2013b. The "Shackleton Site" (IODP site U1385) on the Iberian margin. Proceedings of the Integrated Ocean Drilling Program 16, 13–19. http://dx.doi.org/10.5194/sd-16-13-2013.

Hurrell, J.W., 1995. Decadal trends in the North Atlantic Oscillation: regional temperatures and precipitation. Science 269, 676–679. http://dx.doi.org/10.1126/science.269.5224.676.

IPCC, 2013. Climate change 2013: the physical science basis. In: Stocker, T.F., Qin, D., Plattner, G.-K., Tignor, M., Allen, S.K., Boschung, J., Nauels, A., Xia, Y., Bex, V., Midgley, P.M. (Eds.), Contribution of Working Group I to the Fifth Assessment Report of the Intergovernmental Panel on Climate Change. Cambridge University Press, Cambridge, United Kingdom and New York, NY, USA, p. 1535. http://dx.doi.org/10.1017/CBO9781107415324.

Jouzel, J., Masson-Delmotte, V., Cattani, O., Dreyfus, G., Falourd, S., Hoffmann, G., Minster, B., Nouet, J., Barnola, J.M., Chappellaz, J., Fischer, H., Gallet, J.C., Johnsen, S., Leuenberger, M., Loulergue, L., Luethi, D., Oerter, H., Parrenin, F., Raisbeck, G., Raynaud, D., Schilt, A., Schwander, J., Selmo, E., Souchez, R., Spahni, R., Stauffer, B., Steffensen, J.P., Stenni, B., Stocker, T.F., Tison, J.L., Werner, M., Wolff, E.W., 2007. Orbital and millennial Antarctic climate variability over the past 800,000 years. Science 317, 793–796. http://dx.doi.org/10.1126/science.1141038.

Juggins, S., 2009. Package "rioja" – Analysis of Quaternary Science Data. The Comprehensive R Archive Network.

Koutsodendris, A., Brauer, A., Pälike, H., Müller, U.C., Dulski, P., Lotter, A.F., Pross, J., 2011. Sub-decadal- to decadal-scale climate cyclicity during the Holsteinian interglacial (MIS 11) evidenced in annually laminated sediments. Climate of the Past 7, 987–999. http://dx.doi.org/10.5194/cp-7-987-2011.

Koutsodendris, A., Müller, U.C., Pross, J., Brauer, A., Kotthoff, U., Lotter, A.F., 2010. Vegetation dynamics and climate variability during the Holsteinian interglacial based on a pollen record from Dethlingen (northern Germany). Quaternary Science Reviews 29, 3298–3307. http://dx.doi.org/10.1016/j.quascirev.2010.07.024.

Koutsodendris, A., Pross, J., Müller, U.C., Brauer, A., Fletcher, W.J., Kühl, N., Kirilova, E., Verhagen, F.T.M., Lücke, A., Lotter, A.F., 2012. A short-term climate oscillation during the Holsteinian interglacial (MIS 11c): an analogy to the 8.2ka climatic event? Global and Planetary Change 92–93, 224–235. http://dx.doi.org/10.1016/j.gloplacha.2012.05.011.

Lionello, P., Malanotte-Rizzoli, P., Boscolo, R., Alpert, P., Artale, V., Li, L., Luterbacher, J., May, W., Trigo, R., Tsimplis, M., Ulbrich, U., Xoplaki, E., 2006. The Mediterranean climate: an overview of the main characteristics and issues. Developments in Earth and Environmental Sciences 4, 1–26. http://dx.doi.org/10.1016/S1571-9197(06)80003-0.

Lisiecki, L.E., Raymo, M.E., 2005. A Pliocene–Pleistocene stack of 57 globally-distributed benthic $\delta^{18}O$ records. Paleoceanography 20, PA1003. http://dx.doi.org/10.1029/2004PA001071.

Loidi, J., Biurrun, I., Campos, J.A., Garcıa-Mijangos, I., Herrera, M., 2007. A survey of heath vegetation of the Iberian Peninsula and Northern Morocco: a biogeographical and bioclimatic approach. Phytocoenologia 37, 341–370.

Loutre, M.F., Berger, A.L., 2003. Marine Isotope Stage 11 as an analogue for the present interglacial. Global and Planetary Change 36, 209–217. http://dx.doi.org/10.1016/S0921-8181(02)00186-8.

Magri, D., 2012. Quaternary history of *Cedrus* in southern Europe. Annali Di Botanica 57–66. http://dx.doi.org/10.4462/annbotrm-10022.

Maiorano, P., Marino, M., Balestra, B., Flores, J.-A., Hodell, D.A., Rodrigues, T., 2015. Coccolithophore variability from the Shackleton site (IODP site U1385) through MIS 16-10. Global and Planetary Change 133, 35–48. http://dx.doi.org/10.1016/j.gloplacha.2015.07.009.

Margari, V., Skinner, L.C., Tzedakis, P.C., Ganopolski, A., Vautravers, M., Shackleton, N.J., 2010. The nature of millennial-scale climate variability during the past two glacial periods. Nature Geoscience 3, 127–131.

Marino, M., Maiorano, P., Tarantino, F., Voelker, A., Capotondi, L., Girone, A., Lirer, F., Flores, J.A., Naafs, B.D.A., 2014. Coccolithophores as proxy of seawater changes at orbital-to-millennial scale during middle Pleistocene Marine Isotope Stages 14-9 in North Atlantic core MD01-2446. Paleoceanography 29, 518–532. http://dx.doi.org/10.1002/2013PA002574.

Martrat, B., Grimalt, J.O., Lopez-Martinez, C., Cacho, I., Sierro, F.J., Flores, J.A., Zahn, R., Canals, M., Curtis, J.H., Hodell, D.A., 2004. Abrupt temperature changes in the western Mediterranean over the past 250,000 years. Science 306 (5702), 1762–1765. http://dx.doi.org/10.1126/science.1101706.

Martrat, B., Grimalt, J.O., Shackleton, N.J., de Abreu, L., Hutterli, M.A., Stocker, T.F., 2007. Four climate cycles of recurring deep and surface water destabilizations on the Iberian margin. Science 317, 502–507. http://dx.doi.org/10.1126/science.1139994.

McAndrews, J.H., King, J., 1976. Pollen of the North American Quaternary: the top twenty. Geoscience and Man 15, 41–49.

McManus, J., Oppo, D., Cullen, J., Healey, S., 2003. Marine Isotope Stage 11 (MIS 11): analog for Holocene and future climate? In: Droxler, A.W., Poore, R.Z., Burckle, L.H. (Eds.), Earth's Climate and Orbital Eccentricity: the Marine Isotope Stage 11 Question, AGU Geophysical Monograph Series No. 137, pp. 61–66.

McManus, J.F., Oppo, D.W., Cullen, J.L., 1999. A 0.5-million-year record of millennial-scale climate variability in the North Atlantic. Science 283, 971–974.

Melles, M., Brigham-Grette, J., Minyuk, P.S., Nowaczyk, N.R., Wennrich, V., DeConto, R.M., Anderson, P.M., Andreev, A.A., Coletti, A., Cook, T.L., Haltia-Hovi, E., Kukkonen, M., Lozhkin, A.V., Rosen, P., Tarasov, P., Vogel, H., Wagner, B., 2012. 2.8 million years of Arctic climate change from Lake El'gygytgyn, NE Russia. Science 337, 315–320. http://dx.doi.org/10.1126/science.1222135.

Milker, Y., Rachmayani, R., Weinkauf, M.F.G., Prange, M., Raitzsch, M., Schulz, M., Kučera, M., 2013. Global and regional sea surface temperature trends during Marine Isotope Stage 11. Climate of the Past 9, 2231–2252. http://dx.doi.org/10.5194/cp-9-2231-2013.

Moffa-Sánchez, P., Born, A., Hall, I.R., Thornalley, D.J.R., Barker, S., 2014. Solar forcing of North Atlantic surface temperature and salinity over the past millennium. Nature Geoscience 7, 275–278. http://dx.doi.org/10.1038/ngeo2094.

Moore, P.D., Webb, J.A., Collinson, M.E., 1991. Pollen Analysis, second ed. Blackwell scientific publication, Oxford, p. 216.

Mudie, P., McCarthy, F., 2006. Marine palynology: potentials for onshore—offshore correlation of Pleistocene—Holocene records. Transactions of the Royal Society of South Africa 61, 139–157.

Müller, P.J., Kirst, G., Ruhland, G., Von Storch, I., Rosell-Melé, A., 1998. Calibration of the alkenone paleotemperature index Uk'_{37}- based on core-tops from the eastern South Atlantic and the global ocean (60°N-60°S). Geochimica et Cosmochimica Acta 62, 1757–1772.

Naughton, F., Sánchez Goñi, M.F., Desprat, S., Turon, J.L., Duprat, J., Malaizé, B., Joli, C., Cortijo, E., Drago, T., Freitas, M.C., 2007. Present-day and past (last 25 000 years) marine pollen signal off western Iberia. Marine Micropaleontology 62, 91–114. http://dx.doi.org/10.1016/j.marmicro.2006.07.006.

Naughton, F., Sánchez Goñi, M.F., Kageyama, M., Bard, E., Cortijo, E., Desprat, S., Duprat, J., Malaizé, B., Joli, C., Rostek, F., Turon, J.-L., 2009. Wet to dry climatic trend in north western Iberia within Heinrich events. Earth and Planetary Science Letters 284, 329–342.

Oort, A.H., Vander Haar, T.H., 1976. On the observed annual cycle in the ocean-atmosphere heat balance over the northern hemisphere. Journal of Physical Oceanography 6, 781–800.

Oppo, D.W., McManus, J.F., Cullen, J.L., 1998. Abrupt climate events 500,000 to 340,000 years ago: evidence from subpolar North Atlantic sediments. Science 279, 1335–1338.

Ortega, P., Lehner, F., Swingedouw, D., Masson-Delmotte, V., Raible, C.C., Casado, M., Yiou, P., 2015. A model-tested North Atlantic Oscillation reconstruction for the past millennium. Nature 523, 71–74. http://dx.doi.org/10.1038/nature14518.

Palumbo, E., Flores, J.-A., Perugia, C., Petrillo, Z., Voelker, A.H.L., Amore, F.O., 2013. Millennial scale coccolithophore paleoproductivity and surface water changes between 445 and 360ka (Marine Isotope Stages 12/11) in the Northeast Atlantic. Palaeogeography, Palaeoclimatology, Palaeoecology 383–384, 27–41. http://dx.doi.org/10.1016/j.palaeo.2013.04.024.

Peinado Lorca, M., Martinez-Parras, J.M., 1987. Castilla-La Mancha. In: Peinado Lorca, M., Rivas-Martinez, S. (Eds.), La vegetación de España. Universidad de Alcala de Henares, Alcala de Henares, pp. 163–196.

Peliz, Á., Dubert, J., Santos, A.M.P., Oliveira, P.B., Le Cann, B., 2005. Winter upper ocean circulation in the western Iberian basin – fronts, eddies and poleward flows: an overview. Deep-Sea Research Part I 52 (4), 621–646. http://dx.doi.org/10.1016/j.dsr.2004.11.005.

Peterson, G.M., 1983. Recent pollen spectra and zonal vegetation in the western USSR. Quaternary Science Reviews 2 (4), 281–321.

Pol, K., Debret, M., Masson-Delmotte, V., Capron, E., Cattani, O., Dreyfus, G., Falourd, S., Johnsen, S., Jouzel, J., Landais, A., Minster, B., Stenni, B., 2011. Links between MIS 11 millennial to sub-millennial climate variability and long term trends as revealed by new high resolution EPICA Dome C deuterium data – a comparison with the Holocene. Climate of the Past 7, 437–450. http://dx.doi.org/10.5194/cp-7-437-2011.

Poli, M.S., Thunnel, R.C., Rio, D., 2000. Millennial-scale changes in North Atlantic deep water circulation during Marine Isotope Stages 11 and 12: linkage to Antarctic climate. Geology 28, 807–810.

Polunin, O., Walters, M., 1985. A Guide to the Vegetation of Britain and Europe. Oxford University Press, New York, 238 pp.

Prentice, L.C., 1978. Modern pollen spectra from lake sediments in Finland and Finnmark, north Norway. Boreas 7, 131–153.

Prokopenko, A.A., Bezrukova, E.V., Khursevich, G.K., Solotchina, E.P., Kuzmin, M.I., Tarasov, P.E., 2010. Climate in continental interior Asia during the longest interglacial of the past 500 000 years: the new MIS 11 records from Lake Baikal, SE Siberia. Climate of the Past 6, 31–48. http://dx.doi.org/10.5194/cp-6-31-2010.

Quezel, P., 2002. Réflexions sur l'évolution de la flore et de la végétation au Maghreb méditerranéen. Ibis Press, Paris.

R Core Team, 2014. R: a Language and Environment for Statistical Computing. R Foundation for Statistical Computing, Vienna, Austria. http://www.R-project.org/.

Railsback, L.B., Gibbard, P.L., Head, M.J., Voarintsoa, N.R.G., Toucanne, S., 2015. An optimized scheme of lettered marine isotope substages for the last 1.0 million years, and the climatostratigraphic nature of isotope stages and substages. Quaternary Science Reviews 111, 94–106. http://dx.doi.org/10.1016/j.quascirev.2015.01.012.

Raymo, M.E., Mitrovica, J.X., 2012. Collapse of polar ice sheets during the stage 11 interglacial. Nature 483, 453–456. http://dx.doi.org/10.1038/nature10891.

Raynaud, D., Barnola, J.-M., Souchez, R., Lorrain, R., Petit, J.-R., Duval, P., Lipenkov, V.Y., 2005. Palaeoclimatology: the record for marine isotopic stage 11. Nature 436, 39–40. http://dx.doi.org/10.1038/43639b.

Reille, M., 1992. Pollen et spores d'Europe et d'Afrique du Nord. Laboratoire de botanique historique et palynologie, Marseille, p. 520.

Reille, M., Beaulieu, J.-L. De, Svobodova, H., Andrieu-Ponel, V., Goeury, C., 2000. Pollen analytical biostratigraphy of the last five climatic cycles from a long continental sequence from the Velay region (Massif Central, France). Journal of Quaternary Science 15, 665–685.

Reyes, A.V., Carlson, A.E., Beard, B.L., Hatfield, R.G., Stoner, J.S., Winsor, K., Welke, B., Ullman, D.J., 2014. South Greenland ice-sheet collapse during marine isotope stage 11. Nature 510, 525–528. http://dx.doi.org/10.1038/nature13456.

Roberts, D.L., Karkanas, P., Jacobs, Z., Marean, C.W., Roberts, R.G., 2012. Melting ice sheets 400,000 yr ago raised sea level by 13 m: past analogue for future trends. Earth and Planetary Science Letters 357–358, 226–237. http://dx.doi.org/10.1016/j.epsl.2012.09.006.

Roche, D.M., Wiersma, A.P., Renssen, H., 2010. A systematic study of the impact of freshwater pulses with respect to different geographical locations. Climate Dynamics 34, 997–1013. http://dx.doi.org/10.1007/s00382-009-0578-8.

Rodrigues, T., Grimalt, J.O., Abrantes, F., Flores, J.A., Lebreiro, S., 2009. Holocene interdependences of changes in sea surface temperature, productivity and fluvial inputs in the Iberian continental shelf (Tagus mud patch). Geochemistry, Geophysics, Geosystems 10 (7). http://dx.doi.org/10.1029/2008GC002367.

Rodrigues, T., Voelker, A.H.L., Grimalt, J.O., Abrantes, F., Naughton, F., 2011. Iberian Margin sea surface temperature during MIS 15 to 9 (580–300 ka): glacial suborbital variability versus interglacial stability. Paleoceanography 26. http://dx.doi.org/10.1029/2010PA001927. PA1204.

Rohling, E.J., Grant, K., Bolshaw, M., Roberts, A.P., Siddall, M., Hemleben, C., Kucera, M., 2009. Antarctic temperature and global sea level closely coupled over the past five glacial cycles. Nature Geoscience 2, 500–504. http://dx.doi.org/10.1038/ngeo557.

Roucoux, K.H., Tzedakis, P.C., de Abreu, L., Shackleton, N.J., 2006. Climate and vegetation changes 180,000 to 345,000 years ago recorded in a deep-sea core off Portugal. Earth and Planetary Science Letters 249, 307–325. http://dx.doi.org/10.1016/j.epsl.2006.07.005.

Sánchez Goñi, M.F., Bard, E., Landais, A., Rossignol, L., d'Errico, F., 2013. Air–sea temperature decoupling in western Europe during the last interglacial–glacial transition. Nature Geoscience 6, 837–841. http://dx.doi.org/10.1038/ngeo1924.

Sánchez Goñi, M.F., Cacho, I., Turon, J., Guiot, J., Sierro, F., Peypouquet, J., Grimalt, J., Shackleton, N., 2002. Synchroneity between marine and terrestrial responses to millennial scale climatic variability during the last glacial period in the Mediterranean region. Climate Dynamics 19, 95–105. http://dx.doi.org/10.1007/s00382-001-0212-x.

Sánchez Goñi, M.F., Eynaud, F., Turon, J.L., Shackleton, N.J., 1999. High resolution palynological record off the Iberian margin: direct land-sea correlation for the last interglacial complex. Earth and Planetary Science Letters 171, 123–137.

Sánchez Goñi, M.F., Landais, A., Fletcher, W.J., Naughton, F., Desprat, S., Duprat, J., 2008. Contrasting impacts of Dansgaard-Oeschger events over a western European latitudinal transect modulated by orbital parameters. Quaternary Science Reviews 27, 1136–1151. http://dx.doi.org/10.1016/j.quascirev.2008.03.003.

Sánchez Goñi, M.F., Loutre, M.F., Crucifix, M., Peyron, O., Santos, L., Duprat, J., Malaizé, B., Turon, J.L., Peypouquet, J.P., 2005. Increasing vegetation and climate gradient in western Europe over the last glacial inception (122–110 ka): data-model comparison. Earth and Planetary Science Letters 231, 111–130. http://dx.doi.org/10.1016/j.epsl.2004.12.010.

Sánchez Goñi, M.F., Turon, J.L., Eynaud, F., Gendreau, S., 2000. European climatic response to millennial-scale changes in the atmosphere-ocean system during the last glacial period. Quaternary Research 54, 394–403. http://dx.doi.org/10.1006/qres.2000.2176.

Sánchez-Goñi, M.F., Landais, A., Cacho, I., Duprat, J., Rossignol, L., 2009. Contrasting intrainterstadial climatic evolution between high and middle North Atlantic latitudes: a close-up of Greenland interstadials 8 and 12. Geochemistry, Geophysics, Geosystems 10. http://dx.doi.org/10.1029/2008GC002369.

Santini, M., Collalti, A., Valentini, R., 2014. Climate change impacts on vegetation and water cycle in the Euro-Mediterranean region, studied by a likelihood approach. Regional Environmental Change 14, 1405–1418. http://dx.doi.org/10.1007/s10113-013-0582-8.

Shackleton, N., Fairbanks, R., Chiu, T., Parrenin, F., 2004. Absolute calibration of the Greenland time scale: implications for Antarctic time scales and for Δ14C. Quaternary Science Reviews 23, 1513–1522. http://dx.doi.org/10.1016/j.quascirev.2004.03.006.

Shackleton, N.J., Hall, M.A., Vincent, E., 2000. Phase relationships between millennial-scale events 64,000-24,000 years ago. Paleoceanography 15, 565–569. http://dx.doi.org/10.1029/2000PA000513.

Shackleton, N.J., Sánchez-Goñi, M.F., Pailler, D., Lancelot, Y., 2003. Marine Isotope Substage 5e and the Eemian interglacial. Global and Planetary Change 36, 151–155. http://dx.doi.org/10.1016/S0921-8181(02)00181-9.

Skinner, L.C., Shackleton, N.J., 2005. An Atlantic lead over Pacific deep-water change across Termination I: implications for the application of the Marine Isotope Stage stratigraphy. Quaternary Science Reviews 24, 571–580. http://dx.doi.org/10.1016/j.quascirev.2004.11.008.

Sousa, P., Barriopedro, D., Trigo, R.M., Ramos, A.M., Nieto, R., Gimeno, L., Turkman, K.F., Liberato, M.L.R., 2015b. Impact of Euro-Atlantic blocking patterns in Iberia precipitation using a novel high resolution dataset. Climate Dynamics, 1–19. http://dx.doi.org/10.1007/s00382-015-2718-7.

Sousa, P., Trigo, R.M., Pereira, M., Bedia, J., Gutierrez, J.M., 2015a. Different approaches to model future burnt area in the Iberian Peninsula. Agricultural and Forest Meteorology 202, 11–25. http://dx.doi.org/10.1016/j.agrformet.2014.11.018.

Stein, R., Hefter, J., Grützner, J., Voelker, A., Naafs, B.D.A., 2009. Variability of surface water characteristics and Heinrich-like events in the Pleistocene midlatitude North Atlantic ocean: biomarker and XRD records from IODP site U1313 (MIS 16–9). Paleoceanography 24, PA2203. http://dx.doi.org/10.1029/2008pa001639.

Trigo, R.M., Pozo- Vázquez, D., Osborn, T.J., Castro-Díez, Y., Gamiz-Fortis, S., Esteban-Parra, M.J., 2004. North Atlantic oscillation influence on precipitation, river flow and water resources in the Iberian Peninsula. International Journal of Climatology 24, 925–944. http://dx.doi.org/10.1002/joc.1048.

Tye, G.J., Sherriff, J., Candy, I., Coxon, P., Palmer, A., McClymont, E.L., Schreve, D.C., 2016. The $\delta^{18}O$ stratigraphy of the Hoxnian lacustrine sequence at Marks Tey, Essex, UK: implications for the climatic structure of MIS 11 in Britain. Journal of Quaternary Science 31, 75–92. http://dx.doi.org/10.1002/jqs.2840.

Tzedakis, P.C., Channell, J.E.T., Hodell, D.A., Kleiven, H.F., Skinner, L.C., 2012. Determining the natural length of the current interglacial. Nature Geoscience 5 (2), 138–142.

Tzedakis, P.C., Roucoux, K.H., de Abreu, L., Shackleton, N.J., 2004. The duration of forest stages in southern Europe and interglacial climate variability. Science 306, 2231–2235. http://dx.doi.org/10.1126/science.1102398.

Tzedakis, P.C., 2010. The MIS 11 – MIS 1 analogy, southern European vegetation, atmospheric methane and the "early anthropogenic hypothesis". Climate of the Past 6, 131–144. http://dx.doi.org/10.5194/cp-6-131-2010.

Tzedakis, P.C., Andrieu, V., De Beaulieu, J.L., Birks, H.J.B., Crowhurst, S., Follieri, M., Hooghiemstra, H., Magri, D., Reille, M., Sadori, L., Shackleton, N.J., Wijmstra, T.A., 2001. Establishing a terrestrial chronological framework as a basis for biostratigraphical comparisons. Quaternary Science Reviews 20, 1583–1592. http://dx.doi.org/10.1016/S0277-3791(01)00025-7.

Tzedakis, P.C., Pälike, H., Roucoux, K.H., de Abreu, L., 2009. Atmospheric methane, southern European vegetation and low-mid latitude links on orbital and millennial timescales. Earth and Planetary Science Letters 277, 307–317. http://dx.doi.org/10.1016/j.epsl.2008.10.027.

Villanueva, J., Grimalt, J.O., Cortijo, E., Vidal, L., Labeyriez, L., 1997a. A biomarker approach to the organic matter deposited in the North Atlantic during the last climatic cycle. Geochimica et Cosmochimica Acta 61, 4633–4646.

Villanueva, J., Pelejero, C., Grimalt, J.O., 1997b. Clean-up procedures for the unbiased estimation of C_{37} alkenone sea surface temperatures and terrigenous n-alkane inputs in paleoceanography. Journal of Chromatography A 757, 145–151.

Voelker, A.H.L., Rodrigues, T., Billups, K., Oppo, D., McManus, J., Stein, R., Hefter, J., Grimalt, J.O., 2010. Variations in mid-latitude North Atlantic surface water properties during the mid-Brunhes (MIS 9–14) and their implications for the thermohaline circulation. Climate of the Past 6, 531–552. http://dx.doi.org/10.5194/cp-6-531-2010.

Walter, H., Breckle, S.-W., 1989. Ecological Systems of the Geobiosphere: 3 Temperate and Polar Zonobiomes of Northern Eurasia. Springer-Verlag, Berlin Heidelberg.

Walter, K., Graf, H.-F., 2002. On the changing nature of the regional connection between the North Atlantic oscillation and sea surface temperature. Journal of Geophysical Research 107 (D17), 4338. http://dx.doi.org/10.1029/2001JD000850.

Wijmstra, T.A., Smit, A., 1976. Palynology of the middle part (30–78 m) of the 120m deep section in Northern Greece (Macedonia). Acta Botanica Neerlandica 25, 297–312.

Wood, S.N., 2006. Generalized Additive Models: an Introduction with R. Chapman and Hall/CRC Press.

Wright, J.H.E., McAndrews, J.H., van Zeist, W., 1967. Modern pollen rain in western Iran, and its relation to plant geography and Quaternary vegetational history. Journal of Ecology 415–443.

Yin, Q.Z., Berger, A., 2012. Individual contribution of insolation and CO_2 to the interglacial climates of the past 800,000 years. Climate Dynamics 38, 709–724. http://dx.doi.org/10.1007/s00382-011-1013-5.

Zuur, A.F., Ieno, E.N., Walker, N., Saveliev, A.A., Smith, G.M., 2009. Mixed Effects Models and Extensions in Ecology with R, Statistics for Biology and Health. Springer New York, New York, NY. http://dx.doi.org/10.1007/978-0-387-87458-6.

Please cite this article in press as: Oliveira, D., et al., The complexity of millennial-scale variability in southwestern Europe during MIS 11, Quaternary Research (2016), http://dx.doi.org/10.1016/j.yqres.2016.09.002